

A review on numerical modelling of flashing flow with application to nuclear safety analysis

Liao, Y.; Lucas, D.;

Originally published:

September 2020

Applied Thermal Engineering 182(2021), 116002

DOI: <https://doi.org/10.1016/j.applthermaleng.2020.116002>

Perma-Link to Publication Repository of HZDR:

<https://www.hzdr.de/publications/Publ-31151>

Release of the secondary publication
on the basis of the German Copyright Law § 38 Section 4.

CC BY-NC-ND

A review on numerical modelling of flashing flow with application to nuclear safety analysis

Yixiang Liao^{a,*}, Dirk Lucas^a

^a*Helmholtz-Zentrum Dresden - Rossendorf, Institute of Fluid Dynamics, Dresden, Germany*

Abstract

The flashing flow is an relevant multiphase phenomenon in many technical applications including nuclear safety analysis, which has been the subject of intense research. Numerical studies have evolved from one-dimensional to multi-dimensional. A variety of methods have been proposed, while a broad consensus was not exiting. The present work aims to present an overview of available models as well their assumptions and limitations by conducting a literature survey. The final focus was put on recent computational fluid dynamics simulations. Some consensus on modelling interfacial slip, phase change mechanism and bubble size is identified. Since flashing scenarios often accompanying with high void fraction and broad bubble size range, a poly-disperse two-fluid model is recommended. Thermal phase change model is superior to pressure phase change, relaxation and equilibrium models for practical flashing problems. Major challenges include improving closure models for interphase transfer, bubble dynamics processes, interfacial area as well two-phase turbulence. For this purpose, high-resolution high quality experimental data are important, which are lacking in many cases. Considering that heterogeneous gas structures often exist in flashing flows, multi-field approaches able to handle different shapes of gas-liquid interface are recommended.

Keywords: computational fluid dynamics, flashing flow, nuclear safety analysis, numerical modelling, literature review

*Corresponding author
Email address: Y.Liao@HZDR.de (Yixiang Liao)

1. Flashing phenomenon and its relevance to nuclear safety

2 Production of steam from water boiling is a familiar process under normal
3 operation of light water nuclear reactors, for example, in the core of Boiling
4 Water Reactors (BWRs) and in the Steam Generator (SG) of the Pressurized
5 Water Reactors (PWRs). In these normal situations, water is heated to sat-
6 uration temperature by a hot structure or heat source, e.g. fuel rods in the
7 core or U-tubes in the SG, and steam as energy carrier drives the turbine gen-
8 erators to produce electricity. On the other hand, phase change from liquid to
9 vapor can be triggered by depressurization under nearly adiabatic conditions.
10 Pressure drop may occur in pipes with varying cross section and enhanced el-
11 evation, in relief valves, breaks or other types of mechanical failures[1]. The
12 pressure-driven phase change can be considered as a spectrum of phase change
13 phenomena with cavitation at the cold end and flashing at the hot end [2, 3]. In
14 the case of hot liquids, the temperature of liquid remains almost constant till the
15 phase change starts, but the saturation temperature drops with the pressure.
16 As the pressure of the liquid reaches the saturation pressure corresponding to
17 its temperature, boiling i.e. formation of vapour bubbles takes place as a result
18 of interfacial heat transfer, but sometimes the pressure has to drop below the
19 saturation point [2]. The bubble growth and vapor generation is predominantly
20 controlled by the heat transfer rate at the liquid-vapor interface. The difference
21 between the saturation pressure and the pressure at boiling inception is often
22 referred to as pressure undershoot characterizing the maximal non-equilibrium
23 between the liquid and vapor phases [4]. Its value depends on the initial tem-
24 perature of liquid, depressurization rate, liquid and vapour properties as well
25 nucleation sites available in the system. The thermally-controlled vaporization
26 process under depressurization is commonly referred to as flashing in the com-
27 munity of nuclear engineering, but more often as flash evaporation in the field
28 of desalination [5–8] and flash boiling in spray atomization [9–12]. The flashing
29 phenomenon has received great interest from various branches, and a review on

30 its application and consequence as well existing experimental, theoretical and
31 numerical studies is given by [13]. Although many industrial processes ben-
32 efit from the flashing phenomenon, for example, steam and spray generation
33 [14, 15], absorption and oxidation [16, 17] as well as desalination for gaining
34 drinking water [18–20], the fast phase change process may have a significant
35 impact on the safety and performance of many devices and systems. Concern-
36 ing nuclear safety analysis, flashing behavior is of key importance in terms of
37 determining the reduction rate of reactor coolant inventory and affecting core
38 thermal-hydraulics during the loss of coolant accident (LOCA), and inducing
39 flow instabilities in passive safety systems driven by natural circulation.

40 *1.1. Flashing-related topics under LOCA conditions*

- 41 • **Critical flow problem:** In the frame of nuclear safety analyses numer-
42 ous researchers have investigated steady-state flashing flows through pipes,
43 nozzles, orifices and other restrictions in relation with critical flow problem
44 [21, 22]. In such flows vaporization develops under a constant pressure dif-
45 ference between the inlet and exit of the pipe. As the exit pressure drops
46 below a critical value, the flow rate doesn't increase anymore, which is re-
47 ferred to as critical (or choked) flow. A large body of literature on both
48 experimental and numerical studies arose in the period from late 1960s to
49 early 2000s, e.g. [23–30] among many others. Most of the efforts are driven
50 by the need of predicting maximal flow rates under critical conditions,
51 since it determines the rate at which coolant inventory leaves the reactor
52 cooling system in LOCAs. Among others the BNL (Brookhaven National
53 Laboratory) experiments on flashing flow in a converging-diverging circu-
54 lar nozzle [26] have been analyzed in many numerical works, e.g. [31–41].
- 55 • **Pipe blowdown transient:** There have been also many experimental
56 and theoretical works on transient two-phase flashing flows under pipe
57 blowdown conditions. The major concern here is the early-stage response
58 of initially subcooled but hot liquid in a pipe or vessel during sudden de-
59 pressurization, including the change of fluid temperature and pressure as

60 well as the inception of flashing and void development. The information
61 is of importance for analyzing the system behaviour and checking over
62 the action of safety and protection systems during the accident. Edwards
63 and O'Brien [42] performed transient blowdown experiment using a 4.09 *m*
64 long 0.073 *m* diameter pipe. The horizontal pipe was filled with pressur-
65 ized heated water, a glass disk at one end was ruptured to initiate the
66 blowdown. The measurements of pressure at several positions as well as
67 void fraction have been used for model validation in a number of numeri-
68 cal works such as [43–45]. Takeda and Toda [46] investigated the pressure
69 behavior in a vertical pipe ruptured at the top end with an initial temper-
70 ature gradient increasing from bottom to top. The case was analyzed by
71 Lafferty et al.[47] and Costa et al.[48] with the RELAP5 and WAHA code,
72 respectively. Similar blowdown experiments were conducted by Lienhard
73 et al. [49], Bartak [50] and others. Instead of analyzing the transient
74 pressure behavior in the tube, the objective of these studies was the study
75 of the nucleation delay phenomenon. Semi-empirical correlations based
76 on the classical nucleation theory and experimental data were derived for
77 determining the pressure undershoot.

- 78 • **Lower plenum flashing:** Although the study of pipe critical flow and
79 blowdown phenomena is a contributing part of the LOCA analysis, the
80 fluid behavior and steam generation in the pressure vessel is as well of great
81 interest in the nuclear safety analysis. It affects directly the core cooling
82 and occurrence of core meltdown. As the downcomer level falls, the ini-
83 tially subcooled lower plenum may exceed saturated conditions and flash,
84 resulting in a surge of two-phase flow upwards through the core to the
85 upper plenum. This may reduce the liquid inventory in the lower plenum
86 and downcomer because of vaporization and entrainment, and may also
87 reduce the reflood driving head and prevent the injected cooling water
88 from entering the downcomer. Nevertheless, the liquid entrained in the
89 steam flowing toward the upper part of the vessel may often give a signifi-

90 cant contribution to the cooling of uncovered fuel rods, both in PWR and
91 BWR systems [51, 52]. Transient two-phase flashing flow in the core or
92 large pipes relative to the phenomenon of counter-current flow limitation
93 (CCFL) is investigated insufficiently, due to the complexity of the incident.
94 Phenomenologically, the flashing effects observed in the lower plenum can
95 also be encountered in control rod guide tubes. Because of different ge-
96 ometry and initial liquid subcooling, the flashing intensity is lower and
97 thus less important than the previous one as far as nuclear reactor safety
98 is considered. Nonetheless, it may affect the core thermal-hydraulic be-
99 haviour in a later stage of LOCA transients [51]. In comparison to pipe
100 critical or blowdown flows mentioned above, investigation on the flashing
101 process occurring inside the vessel is challenging due to the large geometry
102 size as well as complex internals. A limited number of studies were per-
103 formed in this area, and a few large-scale experiments on blowdown effects
104 in the pressure vessels are available, e.g. [53–55]. Recently, Wang et al.
105 [56] studied the two-phase flow instability in a PWR-type small modular
106 reactor under LOCA conditions. The temperature and void fraction tran-
107 sients were measured at four ports in the core and riser, and the pressure
108 drop between these ports as well as between the top and the bottom of
109 the containment was measured through differential pressure drop trans-
110 ducers. Ylönen [57] reviewed existing experiments on large-break LOCA,
111 and concluded that for the purpose of CFD code validation, suitable data
112 such as pressure and void fraction at both axial and radial positions are
113 needed.

114 • **SG tube rupture flashing:** In a PWR steam generator (SG) tubes
115 constitute a large fraction of the reactor primary coolant loop pressure
116 boundary. The SG tubes play an important safety role. Any leakage
117 resulting from SG tube rupture (SGTR) will allow radiation to escape
118 into the non-radioactive side of the plant and likely to environment, the
119 function containment being bypassed [58]. Although the core melt fre-

120 quency resulting from SGTR is low relative to other severe accidents, it
121 is a major accident in the field of nuclear safety considering its direct im-
122 pact on the environment. Coolant flow rate through the break is a key in
123 the analysis of SGTR. Due to high pressure drop through the break, the
124 coolant flashes rapidly and the flow becomes choked or critical. As intro-
125 duced above the critical flow problem has been a subject of intense study
126 both experimentally and theoretically. However, the research in the past
127 mostly focused on blowdown from vessels, large pipes or short nozzles,
128 while SGTR presents a particular class of small-break LOCAs (SBLO-
129 CAs). The width of the crack is in the micrometer range and the length
130 of flow path approximates the thickness of SG tube walls ($\sim 1mm$) [59].
131 Assessment and extension of numerical models is necessary. The over-
132 all system performance of a light water PWR during SGTR events with
133 different number of ruptured tubes and with/without ECCS (Emergency
134 Core Cooling System) was tested in many institutions [60–63].

135 *1.2. Flashing-induced instability (FII)*

136 Passive systems utilizing natural circulation have advantages over active
137 ones, and are frequently adopted in new generation reactors [64]. The passive
138 containment cooling system (PCCS) has been developed as an advanced safety
139 feature, for example, in AP1000 [65], ESBWR[66], iPOWER [67], VVER-1200
140 [68], KERENATM [69], and the Hualong pressurized reactor 1000 (HPR1000)
141 [70]. A major disadvantage of the passive systems is the low driving force, which
142 can lead to instability and safety problems. Due to hydrostatic pressure drop
143 in the riser of natural circulation loop, steam generation by flashing can take
144 place. As the steam bubbles condense in cold parts of the loop, oscillation of
145 flow rate, temperature and pressure can be observed, which is referred to as
146 Flashing-induced instability (FII). The FII phenomenon was first observed by
147 Wissler et al. [71] as they conducted experiments on an open natural circu-
148 lation test loop. Since then, many researchers performed experimental studies
149 on the phenomenon, and a majority part focused on the instability problem

150 in BWR during start-up, e.g. [72–75]. At the start-up condition, the coolant
151 may not reach saturation temperature in the core, where it is heated up, and
152 remain single-phase due to low power. However, because of considerable de-
153 crease in coolant saturation temperature along the flow path, flashing can occur
154 in the adiabatic section above the core, and lead to self-sustained flow oscil-
155 lation in the loop. A flashing-driven passive moderator cooling system was
156 developed at AECL for CANDU reactors. It was shown that the concept was
157 feasible at normal operating power, but caused flow instabilities at low power
158 [76, 77]. Similar phenomena were observed in the PCCS systems mentioned
159 above. Recently, Cloppenborg et al. [78] investigated two-phase phenomena in
160 the KERENATM-CCC (containment cooling condenser) natural circulation sys-
161 tem on the GENEVA test circuit. The riser section is two times longer ($\sim 9m$) in
162 comparison to other natural-circulation systems such as CIRCUS [72], equipped
163 with high time and spatial resolution instrumentation for local void fraction and
164 temperature distribution. Since the late 1980s, many researchers have analyzed
165 the FII using numerical methods, and various analysis codes were adopted such
166 as TRACG [79], FLOCAL [80], RELAP5 [81, 82] and MARS [64, 83]. Lim et
167 al.[64] attempted to develop stability maps for FII using the MARS code. Due to
168 high-frequency transients and complex two-phase processes, high-fidelity mod-
169 elling of FII represents still great challenge and difficulty.

170 **2. Widely-used numerical models for flashing flows**

171 As aforementioned, a large body of literature exists on the numerical study
172 of various flashing scenarios conducted with application to nuclear safety anal-
173 ysis. The simulations progress from one-dimensional to three-dimensional. The
174 models range from simple empirical to mechanistic ones with different levels
175 of sophistication. Concerning whether non-homogeneous non-equilibrium ef-
176 fects are considered, they fall into four main categories (a) homogeneous equi-
177 librium model (HEM), (b) non-homogeneous equilibrium model (NHEM), (c)
178 homogeneous non-equilibrium model (HNEM) and (d) non-homogeneous non-

Models	Features	Subcategory	Reference examples
HEM	equal velocity equal temperature		[84–89]
NHEM	unequal velocity equal temperature	slip ratio model	[27, 28, 84, 90]
		drift-flux model	[91, 92]
		two-fluid model	[21, 93, 94]
HNEM	equal velocity unequal temperature	empirical model	[28, 42, 95–100]
		relaxation model	[101–107]
		delayed equilibrium model	[108, 109]
		physically-based model	[31, 43, 110–112]
NHNEM	unequal velocity unequal temperature	drift-flux model	[30, 32, 102, 113]
		two-fluid model	[81, 114, 115]

Table 1: Overview of numerical models for flashing flows

179 equilibrium model (NHNEM). The term "homogeneous" here means equal ve-
180 locities while "equilibrium" denotes equal temperatures of the liquid and vapor
181 phases. The models in each category differ further in their treatment of the
182 mechanical and thermal non-equilibrium and the applied constitutive models,
183 see Table 1. A brief introduction of these models, and a review on representa-
184 tive one-dimensional numerical works are provided in this section, while three-
185 dimensional simulations are discussed subsequently.

186 2.1. The HEM model

187 As the name suggests, the HEM model simplifies the two-phase flow to a
188 pseudo or an equivalent single-phase one flowing with an average velocity and
189 possessing mean thermodynamic properties, which are obtained by interpolat-
190 ing between the saturated liquid and vapour ones using the equilibrium quality.
191 In order to use well-established single-phase theories, the HEM model was very
192 often used for LOCA analysis around 1950s, for example, available in early ver-

193 sions of the system code RELAP. Among others Leung [116] presented a critical
194 flow model on the basis of HEM assumptions. It works well for long pipes for
195 example with a length exceeding 3.0 inches [84], where the time is sufficient
196 for equilibration between the phases. Many works [84–87] discuss the difference
197 between measured and predicted critical flow rates for short pipes, in which
198 there is insufficient time for the two-phase mixture to proceed to equilibrium.
199 The flow rates predicted by the HEM model are considerably less than those ob-
200 tained experimentally. Deligiannis and Cleaver [112] found that the HEM model
201 is incapable of predicting the earliest stage of a rapid depressurization, where
202 the effect of nucleation and thermal non-equilibrium is of prime importance.
203 Inada [88] and Van Bragt et al. [89] investigated flashing effects and instability
204 mechanisms in a natural circulation BWR using the HEM model. Concerning
205 the flow instability Hu et al. [117] and Podowski [118] reported that the HEM
206 predictions are conservative in comparison with a slip or two-fluid model, be-
207 cause the HEM void fraction is higher. According to [29] in the initial stage of
208 steady-state flashing, when bubbles are small and finely dispersed in the liquid,
209 an assumption of hydrodynamic momentum equilibrium is applicable, however,
210 thermal non-equilibrium has to be considered since the interfacial area available
211 for heat transfer is very limited. As the bubbles grow and void fraction exceeds
212 a value of 0.3, thermal equilibrium may be assumed but slip between the phases
213 becomes important and ignoring it will cause inaccuracies.

214 2.2. *NHEM models*

215 Attou et al. [93] studied the effect of interfacial slip on bubbly flow through
216 a sudden enlargement by analyzing two extreme conditions with maximum or
217 negligible momentum transfer between the two phases, respectively. The for-
218 mer assumption is equivalent to HEM, while the latter was referred to as a
219 momentum frozen model (MFM). It was found that in HEM, due to complete
220 momentum transfer between the phases, the lower inertia of the gas causes the
221 liquid to decelerate faster than in reality, leading to a higher pressure recovery
222 than predicted in experiments. Consequently, the MFM causes the liquid to

223 decelerate slower and hence the pressure recovery predicted is lower than in
224 experiments. Addressing the finite rate of interphase transfers is of importance
225 in analyzing flashing flows especially at the later stage [29]. Most earlier ef-
226 forts have been devoted to developing empirical or theoretical correlations for
227 the velocity (or slip) ratio. The theoretical models for critical flow presented
228 in [27, 28, 84, 90] for long tubes are based on the thermodynamic equilibrium
229 assumption but relax the requirement of equal phase velocities by introducing
230 a slip ratio. The next level of complexity is to use the drift-flux model to char-
231 acterize the effect of the relative motion, which evaluates the void distribution
232 parameter and the vapor drift velocity pure empirically. Hu et al. [91] investi-
233 gated the FII during a BWR reactor start-up using a NHEM model. The vapor
234 generation rate was derived from the mixture energy conservation equation,
235 while the nonhomogeneous velocities of the liquid and vapor was considered us-
236 ing the drift-flux approach. A similar equilibrium approach was used in [92] for
237 the linear stability analysis of a boiling natural circulation loop. On the other
238 hand, Wallis [21] and Bouré [94] disadvised the use of drif-flux models. They
239 warned that the relative motion in a rapidly accelerating/decelerating flow with
240 changing void fraction as well flow pattern is determined by a quite different set
241 of terms from which the derivation of drift-flux correlations is based on. It is
242 important to take into account the mechanical interaction between the phases
243 using a separated flow model or two-fluid model when the flashing flow has to
244 be modelled [93].

245 *2.3. HNEM models*

246 Similar to homogeneity of phase velocities, the validity of assumption about
247 thermal equilibrium is limited. According to Donwar-Zapolski et al. [119], the
248 most important feature of flashing flows is the thermal non-equilibrium effects
249 caused by nucleation delay and limited rate of vapor generation. Flashing starts
250 with some delay until the pressure drops below the saturation line, and the real
251 quality pattern differs essentially from the equilibrium one. This greatly influ-
252 ences the void fraction as well as the pressure and velocity distribution along the

253 flow. Kato et al. [120] presented an equation which gave the relative importance
254 of inertial and thermal effects controlling bubble growth in superheated liquid.
255 It was shown that the model has to capture the non-equilibrium nature of the
256 flow in order to simulate flash boiling accurately [121]. The methods describing
257 thermal non-equilibrium fall in four categories:

- 258 • Empirical models: The HEM model is known to over-predict the vapor
259 generation rate and thus under-predict the flow rate in the critical flow.
260 Henry and his co-workers [28] intended to consider the non-equilibrium
261 effect by introducing a correction factor, which allows only a fraction of
262 the equilibrium vapor generation to occur. The empirical factor was de-
263 rived based on the deviation between the measured flow rate and the HEM
264 prediction, and its expression largely depends on the pipe length to diam-
265 eter ratio. For a slip ratio value of unity the authors presented a simple
266 correlation being a function of equilibrium quality only. It assumes that if
267 the quality exceeds 0.05 thermal equilibrium is achieved. For low qualities
268 the non-equilibrium factor was set to 20 times the equilibrium quality, i.e.
269 $N = 20x_{eq}$. The actual flow rate was estimated as $G_{HEM}/N^{1/2}$, where
270 G_{HEM} is the flow rate obtained from the HEM model. In their homo-
271 geneous model assuming equal phase velocities, Simpson and Silver [95]
272 and Edwards [42] introduced two empirical coefficients to account for the
273 non-equilibrium nucleation process. One is the time-delay for bubble nu-
274 cleation, and the other is the number concentration of bubble nuclei. For
275 sake of simplicity Lackmé [96] assumed that evaporation should start if the
276 pressure falls about 5% below the saturation pressure. To determine the
277 nucleation delay more reliably, many experimental and theoretical works
278 on the determination of pressure-undershoot have been carried out, e.g.
279 [4, 50, 97, 98] among others. Based on the classical homogeneous nu-
280 cleation theory and measurement of pressure-undershoot, semi-empirical
281 correlations were proposed, which have been frequently used in the one-
282 dimensional analysis of flashing critical flows such as [99, 100]. A brief

283
284
285
286
287
288
289
290
291
292
293
294
295
296
297
298
299
300
301
302
303
304
305
306
307
308
309
310
311
312

summary of such models as well their applications was given in [2, 122].

- Relaxation models: The basic idea of the relaxation model is that the actual quality x is lower than the equilibrium one x_e . It increases proportionally to the difference between them during the flashing process. The relaxation model for LOCA analysis was first discussed in [101, 102], where the vapor generation rate is correlated with $x_e - x$. Bilicki and Kestin [103] proposed the homogeneous relaxation model (HRM) by adding a rate equation to the HEM equations. It describes the rate of the actual quality x approaching its local equilibrium value. The necessary coefficient is the relaxation time, which is a function of system pressure, mixture enthalpy and actual quality. Downar-Zapolski et al. [119] derived a correlation for the relaxation time basing on the "Super Moby Dick" experiments on critical flow rates [23]. It is a monotonically decreasing function of void fraction and the non-dimensional pressure difference $(p_{sat}(T_{in}) - p)/p_{sat}(T_{in})$. The HRM model and the relaxation time correlation of [119] has been widely adopted in the computational fluid dynamics modelling of flash-boiling atomization, e.g. [3, 104–107], while less in the nuclear safety analysis. Similar relaxation times may be derived for other thermodynamic parameters, and they may differ. Bilicki et al. [123] presented a method for the evaluation of the relaxation time of interphase heat exchange. Mohammadein [124] derived a formula for the thermal relaxation time by solving energy and relaxation equations analytically, in terms of two-phase mixture between two finite temperatures boundaries.
- Delayed Equilibrium Model (DEM): In comparison to others, the delayed equilibrium model (DEM) is not widely used. For the sake of completeness, it is introduced briefly here. The basic idea of the DEM for describing the flashing flow is that the mixture is composed of three phases, i.e. saturated liquid, saturated vapor and metastable liquid [108]. The third phase is in thermal non-equilibrium with the saturated ones, while the whole mixture is at pressure and mechanical equilibrium. The expansion

313 of the metastable liquid is an isentropic process. In addition to the mixture
314 system of equations, an extra mass balance equation for the metastable
315 liquid phase is solved. De Lorenzo et al. [109] benchmarked the DEM
316 model and other three well-known two-phase critical flow models, namely,
317 the HEM model, the Moody NHEM model [27] and the Henry-Fauske
318 HNEM model [28], against more than 450 experimental data. The results
319 showed that none of the classical models can be considered as a general
320 method for the evaluation of the two-phase critical flow. Although positive
321 results in evaluating the critical mass flow rate of long tubes, HEM fails in
322 predicting the critical pressure. Moody's model is unsuitable under two-
323 phase stagnation conditions. The Henry-Fauske model provides rather
324 good results for nozzles and orifices, but overestimates the critical mass
325 flow in long tubes. On the other hand, DEM exhibits reliable results for
326 the configurations ranging from long and short tubes to narrow slits in
327 terms of both critical pressure and critical mass flux.

328 • Physically-based models: As aforementioned, thermal non-equilibrium
329 processes in a flashing flow concern nucleation and interphase heat trans-
330 fer. Some works consider both of them, while others only the latter by
331 prescribing a constant bubble number density. Despite numerous attempts
332 have been made, limited understanding of the physical phenomena pre-
333 vent from defining the non-equilibrium effects precisely. So, it can happen
334 that the results obtained from a physically-based model are worse than
335 those from a simpler one [21, 125]. The non-equilibrium models can be
336 incorporated with homogeneous, drift-flux or two-fluid models in one or
337 more spatial dimensions. Within the context of a one-dimensional homo-
338 geneous model, Wolfert et al. [43] simulated three blowdown experiments
339 by focusing on the interphase heat transfer, which determines the vapor
340 generation rate. The overall transfer coefficient was calculated by combin-
341 ing the heat diffusion model of Plesset and Zwick [126] and the convection
342 model of Ruckenstein [127] cumulatively. Furthermore, they took into

343 account the turbulence enhancement by introducing an eddy conductiv-
344 ity. The bubble number density was treated as a constant, needed to
345 be adjusted from case to case. For the modelling of flashing flow in a
346 converging-diverging nozzle, Wu et al. [31] attempted to find out the
347 flashing inception location by using the semi-empirical onset correlation
348 of Alamgir and Lienhard [4]. Downstream from the onset location, a con-
349 stant number of bubbles was assumed, and the bubbles initially have the
350 critical size corresponding to the onset pressure. The vapor generation
351 rate was assumed to be limited by heat conduction and calculated from
352 the correlation proposed by Plesset and Zwick [126]. The lack of under-
353 standing of the heterogeneous nucleation process remains one difficulty
354 in the modelling of flashing flows. Rohatgi and Reshotko [110] simulated
355 flashing liquid nitrogen flow in a venturi using a one-dimensional HNEM
356 model. They accounted for heterogeneous nucleation by making analogy
357 to the classical homogeneous nucleation theory with the assumption that
358 nucleation in the bulk is dominant. Two adjustable parameters are con-
359 tained in their model, one being the value of activated nucleation site
360 density and the other being the heterogeneity factor. Blinkov and his
361 co-workers developed a quasi-one-dimensional HNEM model to calculate
362 the behavior of nucleation and flashing in nozzles [111]. Besides the mix-
363 ture conservation equations, one continuity equation for the vapor phase
364 and one transport equation for the bubble number density were solved.
365 Both bulk and wall nucleation phenomena were considered. Heteroge-
366 neous nucleation in the bulk was modelled by assuming a size distribution
367 of pre-existing nucleation sites, and the activated nucleation site density
368 is correlated with the Gibbs number. A cavity model was proposed for de-
369 termination of the nucleation site density, bubble departure diameter and
370 frequency at the wall. Deligiannis and Cleaver[112] considered the effect
371 of homogeneous and heterogeneous nucleation in the frame of a two-fluid
372 model with zero slip between the phases.

373 *2.4. NHNEM models*

374 Besides above homogeneous models, the non-equilibrium effects regarding
375 nucleation and interphase heat transfer are often considered in the context of
376 non-homogeneous models, where the velocity difference between the gas and
377 liquid phases is taken into account by using the drift-flux or two-fluid model.
378 [30, 32, 102, 113]

379 • Drift-flux model: Kroeger [102] applied a non-equilibrium drift flux model
380 to two-phase blowdown experiments. The vapor generation rate was calculated
381 from a relaxation type model, and the vapor drift was considered
382 by the correlations proposed by Zuber and Findlay [128]. Another non-
383 equilibrium drift flux model was presented in Elias and Chambé [113].
384 They assumed that the evaporation rate is governed by interphase heat
385 transfer. The evaporation rate is determined by a conduction bubble
386 growth model[129], while the convection effect is negligible. A similar
387 non-equilibrium model was developed by Saha and his co-workers [30],
388 and the major difference lies in modelling of interphase heat transfer.
389 Saha et al. stated that the Plesset-Zwick or Forster-Zuber type of heat
390 transfer coefficient may be applicable for short time after nucleation. As
391 the bubbles "age", convection starts to dominate the heat transfer because
392 of the relative velocity between the bubbles and liquid. They used a simple
393 expression which provides the root mean square of the conduction and
394 convection heat transfer coefficients [130]. Riznic et al.[32] improved the
395 drift-flux model by considering bubble generation and transportation instead
396 of assuming a constant bubble number density. The bubble number
397 transport equation was solved with a distributed source from wall nucleation.
398 In addition, they took into account the variable pressure effects in their
399 conduction bubble growth model according to the results of Jones
400 and Zuber [131]. They found that in a variable pressure field, which cause
401 the saturation temperature to vary as t^n (t being time), the bubble radius
402 will grow as $t^{n+1/2}$. It is significantly faster than $t^{1/2}$ usually expected for

403
404
405
406
407
408
409
410
411
412
413
414
415

416
417
418
419
420
421
422
423
424
425
426
427
428
429
430

the initial superheat.

- Two-fluid model: Saha et al.[30] recognized that a two-fluid model is superior to the drift-flux model for calculating relative velocity. One-dimensional two-fluid equations were used by Ardron [132] for the calculation of critical flow in a pipe. The nucleation and diffusion-limited growth of vapor bubbles in superheated liquid were considered in the determination of vapor generation rate. The nucleation rate was computed based on the classical nucleation theory by introducing a heterogeneity factor. A similar model was presented in [110], where the density of nucleation sites and the heterogeneity factor are two adjustable parameters. By neglecting the sphericity of the bubble and assuming linear time variation of the liquid superheating degree, the diffusive heat flux from the thermal boundary to the bubble wall was approximated as

$$q_i(t, t') = \frac{\lambda_l}{\sqrt{\pi a_l(t - t')}} [2T_{sup}(t) - T_{sup}(t')] \quad (1)$$

where t' is the time point at which the bubble is created, λ_l and a_l are liquid thermal conductivity and diffusivity. Rivard and Travis [133] described the vapor production and bubble growth by the well-known heat diffusion controlled rate presented in [126], but considered the enhancement in thermal diffusivity due to the effect of relative motion and liquid turbulence, i.e. $a_{eff} = a_l + Ar_B U_{rel}$, where $a_{eff}, a_l, r_B, U_{rel}$ is effective diffusivity, molecular diffusivity, bubble radius and relative velocity, respectively, and A is an empirical constant. In addition, a constant bubble number density $N = 10^9 m^{-3}$ was specified and nucleation was neglected. Richter[29] applied the two-fluid model to calculation of critical flow rates for steam-water mixtures from nozzles. He postulated that convection is the dominant mode of interphase heat transfer during flashing, and adopted the empirical correlation proposed by Ranz and Marshall [134] for estimation of heat transfer coefficient in the bubbly flow regime. Different flow regimes were considered in the model, like bubbly, churn-turbulent

431 and annular. The transition from one regime to another was assumed to
432 occur at certain void fractions. A similar two-fluid model was presented in
433 [125], while different correlations were used for the constitutive equations,
434 i.e. drag coefficient and heat transfer coefficient. Schwellnus [135] included
435 a seventh equation for bubble diameter up to the point from bubbly to
436 churn-turbulent flow. The bubble number density was updated basing on
437 the bubble diameter and void fraction. For the purpose of analyzing crit-
438 ical flows in pipes of nondiverging cross-sectional area, Dagan et al. [136]
439 derived an empirical correlation for the number density of bubbles as a
440 function of pipe's length to diameter ratio. Furthermore, they extended
441 the conduction bubble growth model proposed by Olek et al. [137] to in-
442 clude the convection effects. Tiselj and Petelin [33] simulated the critical
443 flashing flow in a converging-diverging nozzle with the two-fluid model in
444 RELAP5. The simulation results were compared with the experiments
445 performed in the BNL laboratory [26]. They pointed out that the major
446 source of discrepancies is the neglect of the flashing delay. Recently, Koz-
447 menkov et al. [81] and Atajafari et al. [114] validated the RELAP5 code
448 for FII observed at the CIRCUS [72] and SIRIUS-N [73] test facilities ,
449 respectively. Wein [115] developed a two-fluid model for flashing flows of
450 initially subcooled and saturated fluids through pipes and nozzles. It con-
451 sists of six conservation equations of mass and momentum, liquid thermal
452 energy and bubble number transport. Constitutive equations describing
453 interphase mass, momentum and heat transfer account for different flow
454 regimes. Nucleation on the wall and in the bulk flow was considered.
455 The results proved that the importance of fluid dynamic non-equilibrium
456 increases with vapor volume fraction.

457 **3. Computational fluid dynamics modelling**

458 Multi-dimensional CFD-based simulations are becoming a useful tool for
459 studying transients, instabilities and phase transitions in two-phase flow sys-

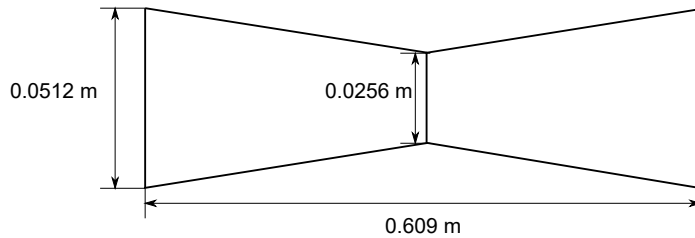


Figure 1: Vertical circular convergent-divergent nozzle in BNL experiments [26]

460 tems [118]. Since the beginning of the 2000s there arise a number of CFD
 461 works on flashing flow related to the nuclear reactor safety problems. Insights
 462 to smaller scale flow processes which were not seen by system codes may be ac-
 463 quired by using the CFD tool. It brings a better understanding of local physical
 464 phenomena, more confidence in the results and then better definition of safety
 465 margins. However, the same problem as in one-dimensional codes encountered
 466 here is that, constitutive models are not as mature as in single phase flows, and
 467 a general consensus regarding model selection is not available. A lot of work
 468 has still to be done on the physical modelling and numerical algorithm [138].

469 3.1. Flashing nozzle flow

470 CFD simulation of flashing flows in nuclear applications are mostly concen-
 471 trated on the steady-state nozzle flow or critical (choked) flow. Considering
 472 that the BNL experiments [26] have been frequently simulated, geometrical de-
 473 tails about the nozzle and some test runs are presented in Figure 1 and Table
 474 2, respectively. In most cases the mass flow rates obtained using different mod-
 475 els conform well with the data, although adjustment of some parameters such
 476 as the accommodation coefficient [41] and the bubble number density [40] was
 477 often necessary. Details about the numerical methods and models adopted in
 478 each work are discussed below.

479 Maksic and Mewes [35] examined the flashing flow in the BNL nozzle [26]
 480 by performing simulations with the commercial CFD-code ANSYS CFX version
 481 4.2. The simplified two-phase model consists of continuity and momentum equa-

Run #	p_{in} [kPa]	p_{out} [kPa]	T_{in} [K]	\dot{m}_{exp} [kg/s]	\dot{m}_{cal} [kg/s]
122	171.0	109.2	373.35	6.12	6.25 [36]
128	248.0	101.0	373.15	9.13	8.78 [36]
133	349.0	203.0	394.35	9.0	9.2 [40] 8.80 [36]
137	464.0	208.9	394.75	11.95	12.1 [40]
145	306.0	208.7	394.35	7.52	7.7 [40] 7.37 [37]
148	304.0	206.0	394.35	7.52	7.50 [36] 7.33 [37]
268	575.2	443	422.05	8.74	8.4 [40] 9.20 [41] 9.10 [139]
273	573.5	442.1	421.85	8.72	8.3 [40], 8.85 [35] 8.51 [37], 9.30 [41]
278	688.6	434.1	421.95	11.67	10.9 [40], 12.30 [41]
284	530.1	456.0	422.35	7.30	7.0 [40], 7.70 [41]
288	530.8	456.3	422.25	7.26	7.12 [37]
291	504.7	470	422.05	6.44	6.1 [40]
296	764.9	432.6	421.95	13.13	12.4 [40], 13.90 [41]
304	577.7	441	422.15	8.76	9.1 [40], 9.10 [41]
309	555.9	402.5	422.25	8.80	8.4 [40], 8.75 [36] 7.56 [37], 8.80 [41] 8.72 [139]
344	539.9	190.0	394.15	13.47	12.7 [40]
348	226.9	199.4	394.35	4.57	4.30 [37]
358	370.2	101.2	373.15	12.13	11.5 [40]
362	443.3	101.2	372.85	13.68	12.9 [40]

Table 2: Operational conditions and test runs in BNL experiments [26]

482 tions for the mixture of liquid and vapor, a separate continuity equation for the
 483 vapor and an energy equation for the liquid. The vapor phase was assumed to
 484 be saturated, and its temperature was calculated from the local pressure. The
 485 four-equation HNEM model was supplemented with a transport equation for the
 486 bubble number density. Both bubble sizes and numbers were allowed to change
 487 in this way. The generation of bubbles from wall nucleation was considered, and
 488 the nucleation rate was calculated according to the Jones model [111, 131]. The
 489 surface source was transformed to a volumetric source by multiplying it with
 490 the ratio of the pipe perimeter to the cross-sectional area of the pipe $\frac{\xi}{A}$, i.e.

$$J_w = N_w f_w \frac{\xi}{A} \quad (2)$$

491 where N_w, f_w denotes the nucleation site density and nucleation frequency at
 492 the wall, respectively. The transformation in Eq. (2) may lead to inconsistency,
 493 since N_w has a value of zero everywhere except in the cells adjacent to the
 494 wall. For the calculation of interfacial area density, the authors considered two
 495 regimes, bubbly regime ($\alpha < 0.3$) and slug regime ($\alpha > 0.3$). In the slug
 496 flow regime, the interfacial area density was assumed to be the sum of that of
 497 spherical bubbles and cylindrical slugs, but the volume fraction of each type
 498 of the bubbles was not provided. The interfacial heat transfer was assumed
 499 to be dominated by heat conduction, and the Nusselt number is a function of
 500 the Jakob number. The empirical correlation presented by Labuntzov [140] was
 501 adopted.

$$Nu = 2 + \frac{12}{\pi} Ja + \left(\frac{6Ja}{\pi} \right)^{1/3} \quad (3)$$

502 The Jakob number is defined by

$$Ja = \frac{c_{pl} \rho_l \Delta T_{sup}}{\rho_v H_{lv}} \quad (4)$$

503 where c_{pl} is the isobaric heat capacity of liquid. For the test run 273 with
 504 inlet pressure of 573.5 *kPa*, temperature of 421.85 *K*, see Table 2, a good
 505 agreement on the mass flow rate was achieved. However, the simulation showed

506 a fluctuating pressure profile in the diverging part of the nozzle, and under-
 507 predicted the void fraction in the diverging part of the nozzle.

508 Marsh and O’Mahony [37] simulated the same nozzle flow using a full two-
 509 fluid model in the commercial CFD code ANSYS FLUENT, with separate mass,
 510 momentum and enthalpy balance equations for liquid and vapour. Inter-phase
 511 mass and momentum as well as energy transfer resulting from both nucleation
 512 and phase change were taken into account. However, the effect of non-drag forces
 513 on the momentum exchange and heat transfer between the vapor and vapor-
 514 liquid interfaces were neglected. Like in the previous work vapor generation
 515 is determined from interphase heat transfer, but information about the heat
 516 transfer coefficient is not provided. The generation of bubbles from nucleation
 517 was taken into account by solving a bubble transport equation. The nucleation
 518 rate was computed by a modified version of the Blander and Katz model [141].

$$J_w = N^{2/3} S \left(\frac{2\sigma N_A}{\pi m_w B} \right)^{1/2} \exp \left(- \frac{\phi}{(T_{sat} - T_l)^n} \right) \quad (5)$$

519 where N is the number of liquid molecules per unit volume, and the power $2/3$
 520 is to transform it to a surface density, m_w is the molecular weight and $S = (1 -$
 521 $m_w)/2$, N_A is the Avogadro number, σ is the surface tension coefficient, and B
 522 is a constant having a value of $2/3$ in case of flashing. The exponential term was
 523 written in terms of superheat instead of pressure undershoot as in the original
 524 model for the sake of numerical stability. In addition to the heterogeneous
 525 factor ϕ an adjustable constant n was introduced. Details on how to convert
 526 the surface flux J_w to the volumetric source required by the bubble transport
 527 equation are not provided. The calculated and measured mass flow rate was
 528 compared for six BNL runs carried out by Abuaf et al. [26], see Table 2. Good
 529 agreement was achieved for all cases except Run 309, which has a high inlet
 530 pressure and a relatively low outlet pressure, in other words high vaporization
 531 rate. Furthermore, in contrast to that a bubble layer in the vicinity of the wall
 532 as reported in [35], the distribution of vapor in the diverging part of the nozzle
 533 is almost uniform. The difference mainly results from the nucleation models

534 that are applied. The model of Blander and Katz [141] was derived from the
 535 classical nucleation theory for bulk nucleation and activated not only on the
 536 walls but all over the domain depending on local liquid superheat. It differs in
 537 nature from the Jones wall cavity model [111] used in the previous work.

538 The disagreement on nucleation modelling motivated Janet et al. [39] to
 539 evaluate the existing models. They analyzed the heterogeneous nucleation ef-
 540 fects in the BNL nozzle using the two-fluid model in ANSYS CFX 15.0. As in
 541 the work of Maksic and Mewes [35], the vapor and vapor-liquid interface were
 542 assumed to remain saturated by applying the zero resistance model, but sepa-
 543 rate velocity fields were solved for the liquid and vapor phases. To estimate the
 544 heat transfer between the superheated liquid and the interface, the correlation
 545 of Aleksandrov [142] was used. It combines the heat diffusion and convection in
 546 the following way:

$$Nu = \left(\frac{12}{\pi^2} Ja_T^2 + \frac{1}{3\pi} Pe \right)^{1/2} \quad (6)$$

547 where Pe is the Péclet number. Like in [35, 37] a transport equation was solved
 548 additionally for the bubble number density. The nucleation source was imple-
 549 mented as a boundary flux into the near-wall mesh cells. Three wall nucleation
 550 models, i.e. the Jones model [111, 131], the RPI model [143] and Riznic model
 551 [32], were investigated. The performance of the models was found to differ qual-
 552 itatively and quantitatively in predicting of the bubble departure frequency and
 553 diameter along the nozzle. The Jones model predicted the best agreement on
 554 the mass flow rate. Considering only wall nucleation leads to the same profile
 555 as observed in [35], i.e. a bubble layer appearing in the vicinity of the wall,
 556 whose thickness increases along the nozzle axis, while the void fraction in the
 557 central part of the nozzle is nearly zero. On the other hand, the measured pro-
 558 files show non-zero values in the central region along with high peaks near the
 559 wall. Based on this observation, Janet et al. [39] suggested that both wall and
 560 bulk nucleation play a role in flashing nozzle flows although wall nucleation is
 561 dominant in most cases. The effect of bulk nucleation was considered by using

562 the model proposed by Rohatgi and Reshotko [110]. The bulk nucleation rate
 563 is given by

$$J_b = N_b \left(\frac{2\sigma}{\pi m_w} \right)^{1/2} \exp \left(- \frac{16\pi\sigma^3\phi}{3\kappa T_l (p_{sat} - p_l)^2} \right) \quad (7)$$

564 where N_b is the number density of liquid molecules, p_{sat} is the vapor pressure
 565 at the liquid temperature and κ is the Boltzmann constant. Considering both
 566 wall and bulk nucleation improves the agreement between the measured and
 567 simulated radial profiles considerably.

568 The nucleation region in above BNL nozzle test runs has been shown suffi-
 569 ciently narrow (a few centimeters) both experimentally [31] and numerically [39].
 570 The bubble number density is nearly constant after the nucleation region. Based
 571 on these observations Liao and Lucas [40] revisited these cases with prescription
 572 of the bubble number density. The initial tiny bubbles can be deemed as pre-
 573 existing germs, which start to grow as long as the surrounding liquid becomes
 574 saturated. This is a major difference from the numerical model applied in the
 575 previous work of [39], where the nucleation delay was considered. Fourteen cases
 576 with different inlet/outlet pressures and temperatures were benchmarked. The
 577 error between predicted mass flow rates and experimental data for all cases was
 578 below 7%, see Table 2. At the same time, satisfying agreement regarding axial
 579 profiles of void fraction and pressure was observed, which are greatly improved
 580 in comparison with the one-dimensional results published in [31]. However,
 581 the lateral distribution of bubbles reveals large discrepancy, although non-drag
 582 forces including lift, added mass, turbulence dispersion and wall lubrication are
 583 considered [144]. Both simulation and experiment gives a wall-peak profile,
 584 but the predicted void fraction in the central region is much too high. It evi-
 585 denced that dynamic processes such as bubble nucleation, growth, coalescence
 586 and breakup were not reproduced by the numerical model appropriately, apart
 587 from the uncertainties in the force models. To capture the lateral bubble migra-
 588 tion, a poly-disperse approach tracing the local bubble size change is necessary.

589 Mimouni et al. [145] simulated one critical flow case of the Super Moby

590 Dick experiment [146] with the NEPTUNE_CFD solver. It has the boundary
 591 conditions of 39.96 bars at the inlet and 23.176 bars at the outlet, and the initial
 592 water subcooling is of about 10°C. Mass, momentum and energy balance equa-
 593 tions are solved for both liquid and vapor. The interfacial transfer of momentum
 594 consisted of three forces, i.e. drag, virtual mass and the secondary momentum
 595 source associated with the interfacial mass transfer. Nucleation occurring at the
 596 wall and pre-existing germs are considered. The former is modelled by using
 597 the Jones nucleation model [111], while the latter by presuming an initial void
 598 fraction. In addition, the original correlation for the nucleation site density was
 599 modified for sake of generality. The change of bubble size and number density
 600 was not solved, and instead, a constant value was prescribed for the bubble size.
 601 The heat transfer coefficient on the vapor side was set to a large value to ensure
 602 the vapor temperature remaining very close to the saturation temperature, and
 603 on the liquid side was calculated using the Ranz-Marshall correlation [134].

$$Nu = 2.0 + 0.6Re_p^{1/2}Pr_l^{1/3} \quad (8)$$

604 While the majority of investigations indicated that the wall nucleation is
 605 predominant in flashing flows, Mimouni et al. [145] found the vapor genera-
 606 tion at the wall negligible in comparison to that from pre-existing nuclei. The
 607 inconsistency is caused by the fact that the pre-existing nuclei are activated
 608 earlier (at saturation conditions) and suppress the activation of nuclei on the
 609 walls. It can be expected that the void fraction in the central region would be
 610 over-predicted as shown in [40]. The effect of initial void fraction as well bubble
 611 size was discussed. Taking into account the poly-dispersity was identified as one
 612 important issue requiring further efforts.

613 In all above investigations phase change was deemed driven by thermal dif-
 614 ference, and the bubble growth and vapor generation rate was determined by
 615 modelling the interfacial heat transfer process. Similar for nucleation models,
 616 a broad consensus on choosing interphase heat transfer models does not ex-
 617 ist. In some works conduction was assumed to be a predominant heat transfer

618 mechanism, while in others convection. An evaluation of the heat transfer coef-
619 ficient models for flashing flows was conducted by Liao and Lucas [130]. They
620 attempted to generalize the model by taking into account convection and tur-
621 bulence effects along with the conduction, and validated it for condensing and
622 evaporating flows [130, 147].

623 On the other hand, a few CFD works on the flashing nozzle flow assumed
624 that phase change is controlled by pressure difference, and applied a conven-
625 tional cavitation model derived from the R-P (Rayleigh-Plesset) equation. For
626 example, Palau-Salvador et al. [36] simulated the BNL nozzle flow [26] using
627 the cavitation model of Singhal et al. [148] available in the CFD code ANSYS
628 FLUENT 6.1. The model assumes that the flow is isothermal. Pre-existing
629 germs start to grow as local pressure drops below the saturation pressure, and
630 collapse in the reverse case. Mass and momentum balance equations are solved
631 for the mixture of liquid and vapor. Like in [35], a transport equation was
632 solved for the vapor fraction besides the mixture conservation equation, and the
633 source terms representing bubble growth and collapse are described by the R-P
634 equation.

$$\dot{\Gamma} = \begin{cases} C_{vap} \frac{\max(1.0, \sqrt{k})(1 - f_v - f_g)}{\sigma} \rho_l \rho_v \sqrt{\frac{2(p_v - p)}{3\rho_l}} & \text{if } p \leq p_v, \\ -C_{cond} \frac{\max(1.0, \sqrt{k})f_v}{\sigma} \rho_l \rho_l \sqrt{\frac{2(p - p_v)}{3\rho_l}} & \text{if } p > p_v. \end{cases} \quad (9)$$

635 Wherein f_v, f_g are mass fraction of vapor and non-condensable gases, k is tur-
636 bulent kinetic energy, C_{vap}, C_{cond} are two empirical coefficients having a unit
637 of m/s . The local turbulence effect on the saturation pressure is considered by
638 considering an additional turbulent fluctuation:

$$p_v = p_{sat} + 0.195\rho k \quad (10)$$

639 Five BNL test runs from [26] were validated, see Table 2. Good agreement
640 between the measured and calculated mass flow rates was achieved with a dif-
641 ference less than 4%. Satisfying prediction of axial pressure and vapor fraction

642 was shown for one case, where the thermal non-equilibrium effect at the onset
643 of flashing is not that significant. As expected from the homogeneous mixture
644 model, the contour plot of void fraction exhibits a uniform distribution of vapor
645 in the lateral direction of the nozzle, which is inconsistent with the experimen-
646 tal observation as discussed above. Another cavitation model in the ANSYS
647 FLUENT code, i.e. the Schnerr and Sauer model [149], was utilized by Ishigaki
648 et al. [150] for analyzing the two-phase critical flow in nozzles and breaks. The
649 Super Moby Dick experiment [146] and the SGTR experiment at Large Scale
650 Test Facility (LSTF) of Japan Atomic Energy Agency [151] were simulated.
651 The authors concluded that the CFD code ANSYS FLUENT has the possibil-
652 ity for simulation of two-phase critical flows related nuclear safety analysis. The
653 physical properties were shown to have a significant influence on the flow rate
654 predictions, and an more accurate estimation is necessary. The authors treated
655 the vapor as an ideal gas, and calculated the density of liquid according to the
656 Tait equation of state. In contrast, the simulations performed in ANSYS CFX
657 mostly use the IAPWS-IF97 formulation of the thermodynamic properties of
658 water and steam.

659 On the other hand, Liu et al. [38] pointed out that above isothermal cavitat-
660 ion models cannot be used for flashing flows directly, because the dependency
661 of vapor generation rate on temperature variations is usually non-negligible
662 under the high temperature and pressure conditions. They constructed a so-
663 called thermodynamic cavitation model based on the homogeneous multiphase
664 model with common flow fields shared by all fluids including temperature and
665 turbulence. In order to take into account the thermal effects in flashing, the
666 dependency of fluid physical properties on the temperature was introduced, e.g.
667 the saturation vapor pressure, surface tension as well liquid and vapor densities,
668 using empirical formulas. The mass transfer source terms related to bubble
669 growth and collapse were derived based on the H-K (Hertz-Knudsen) formula,
670 which gives the evaporation-condensation flux based on the kinetic theory on a

671 flat interface.

$$\dot{\Gamma} = \begin{cases} F_{vap} \frac{6(1-f_v-f_g)}{d_B} \frac{2\sigma}{2-\sigma} \sqrt{\frac{M}{2\pi RT}} (p_v - p) & \text{if } p \leq p_v, \\ -F_{cond} \frac{6f_v}{d_B} \frac{2\sigma}{2-\sigma} \sqrt{\frac{M}{2\pi RT}} (p - p_v) & \text{if } p > p_v. \end{cases} \quad (11)$$

672 where M is the molar mass of liquid, R is the gas constant, T is the mixture
 673 temperature, and F_{vap} , F_{cond} are two adjustable constants. The contribution of
 674 turbulent fluctuation to the pressure variation was considered according to Eq.
 675 (10). The authors simulated one BNL nozzle test run with the modified cavita-
 676 tion model, and compared the simulation results with those presented in [36]. A
 677 minimal improvement of the axial void fraction profile was indicated. Further-
 678 more, it showed surprisingly that the vapor volume fraction at the temperature
 679 of $100^\circ C$ is higher than $150^\circ C$. It implies that the way how the thermal effect
 680 was considered is inappropriate.

681 Le et al. [41] investigated the BNL nozzle flow experiments by implementing
 682 a similar model as [38] in the commercial code ANSYS FLUENT 16.2. The
 683 source term for the mass flux at the interface is derived according to the H-K
 684 formula,

$$\dot{\Gamma} = A_i \beta \sqrt{\frac{M}{2\pi RT_{sat}}} (0.195\rho k + p_{sat} - p^*) \quad (12)$$

685 where β is the so-called "accommodation" coefficient taking into account the
 686 thermal non-equilibrium effects partially. The interfacial area density A_i is
 687 modelled by assuming a constant bubble number density as in [40]. The source
 688 term was inserted by means of a user-defined function. The coefficient β as
 689 well the pressure difference $dp = p_{sat} - p^*$ was treated as adjustable constants
 690 in the simulation. The model was validated against experimental data [26]
 691 and numerical results of previous work [39, 40]. The discrepancies between
 692 the measured and simulated radial vapor profiles were attributed to the two-
 693 phase mixture approach and the slip model, which makes use of an algebraic
 694 slip relation for the relative velocity. A two-fluid model along with a complete

695 modelling of the thermal effects was recommended.

696 In the frame of a homogeneous mixture model Jin et al. [139] included source
 697 and sink terms of interfacial mass transfer induced by both pressure and thermal
 698 difference ($\dot{\Gamma} = \dot{\Gamma}_p + \dot{\Gamma}_T$). The pressure phase change model has a similar form
 699 as Eq. (11) and Eq. (12), i.e.

$$\dot{\Gamma}_p = \begin{cases} F_{vap} \frac{\rho_v f_l}{t_{ch}} \min\left(1, \frac{p_v - p}{k_p p_v}\right) & \text{if } p \leq p_v, \\ -F_{cond} \frac{\rho_v f_v}{t_{ch}} \min\left(1, \frac{p - p_v}{k_p p_v}\right) & \text{if } p > p_v. \end{cases} \quad (13)$$

700 where t_{ch} is the characteristic flow time, k_p is a scaling constant that determines
 701 the pressure level at which the vaporization model comes into effect. The ther-
 702 mal mass transfer rate was calculated according to the thermal phase change
 703 model presented by Lee [152].

$$\dot{\Gamma}_T = \begin{cases} F_{vap} \frac{\rho_l f_l (T - T_v)}{t_{ch} T_v} & \text{if } T > T_v, \\ -F_{cond} \frac{\rho_v f_v (T_v - T)}{t_{ch} T_v} & \text{if } T \leq T_v. \end{cases} \quad (14)$$

704 The model was implemented in a in-house CFD code, whose capability of sim-
 705 ulating flashing flows was assessed by studying the BNL nozzle flow. Two test
 706 runs (309 and 268) were simulated, and good agreement in terms of axial profiles
 707 of pressure and void fraction was achieved.

708 Schmidt et al. [3] extended the classical one-dimensional closures for the
 709 HRM model proposed by Downar-Zapolski et al. [119], to multiple dimensions,
 710 and implemented them in the open source CFD code OpenFOAM. The solver
 711 was firstly validated for a case taken from Tikhonenko et al. [153], who explored
 712 flashing critical flow in various pipes with a sharp inlet. These experiments
 713 include pressure measurements along the length of the pipe. High-pressure and
 714 low-pressure correlations for the relaxation time Θ were tested.

$$\Theta = \begin{cases} 6.51 \times 10^{-4} \alpha^{-0.257} \psi^{-2.24} & \text{if } p \leq 10\text{bar}, \\ 3.84 \times 10^{-7} \alpha^{-0.54} \phi^{-1.76} & \text{if } p > 10\text{bar}. \end{cases} \quad (15)$$

715 where the definitions for ψ and ϕ are

$$\psi = \left| \frac{p_{sat} - p}{p_{sat}} \right| \quad (16)$$

$$\phi = \left| \frac{p_{sat} - p}{p_c - p_{sat}} \right| \quad (17)$$

716 where p_c denotes the critical pressure. Both correlations were found to under-
717 predict the flashing rate, and the low-pressure correlation is especially far off.
718 The second test case was taken from the experiments conducted by Fauske [154],
719 in a relatively short and small tube. In this case, surprising good agreement on
720 the mass flow rate was achieved by the low-pressure correlation, while the high-
721 pressure correlation under-predicted by a factor of two. The authors concluded
722 that future development should focus on developing a general correlation for the
723 relaxation time, and considering non-homogeneous, turbulence and nucleation
724 effects.

725 Similar attempts extending a one-dimensional model to multi-dimensions
726 were made by Duponcheel et al. [155]. They implemented and the DEM model
727 in the NEPTUNE.CFD multi-field solver, and tested it for flashing choked
728 flows. The validation cases were taken from the Super Moby Dick experiments
729 [146]. Two inlet conditions were simulated: $T_{in} = 240.5 \text{ }^\circ\text{C}$ and $T_{in} = 249.4 \text{ }^\circ\text{C}$.
730 The homogeneous condition, i.e. identical velocities for all the phases, is ob-
731 tained by adding very large drag forces. The saturated liquid and vapor were
732 constrained to remain saturated by adding strong interfacial heat transfer terms.
733 The metastable liquid phase was considered "frozen", and no interfacial heat
734 transfer with the saturated phases. The mass transfer from the metastable liq-
735 uid to the saturated liquid was determined by using an empirical correlation.
736 The implemented model was able to give good agreement for the case closer to
737 saturation, but under-predicted the mass flow rate by 13.5% in case of larger
738 inlet subcooling. Yet, in both cases the multi-dimensional results are wors-
739 er than the one-dimensional ones using the original DEM.

740 As shown above various phase-change models have been adopted for the pre-

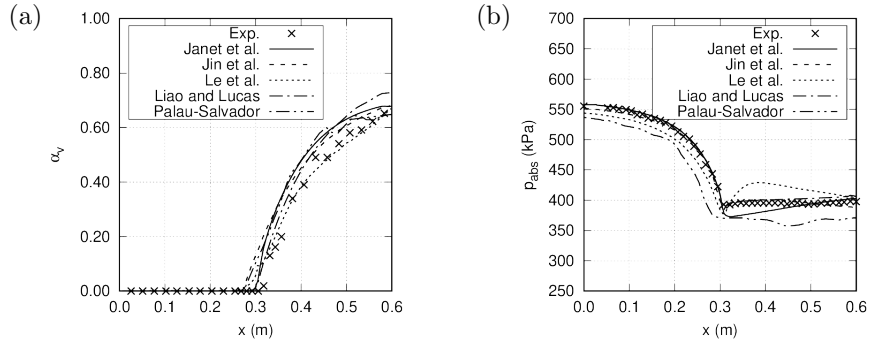


Figure 2: Comparison between simulation results from literature for BNL test case 309 [4].
(a) Axial void fraction profile (b) Axial pressure profile

741 diction of flashing flows, e.g. thermal phase-change model based on temperature
742 difference (TPCM) and pressure phase-change model based on pressure differ-
743 ence (PPCM). The PPCM models can be divided further into two categories,
744 i.e. based on the kinetic theory of gases (H-K equation) and based on bub-
745 ble dynamics (R-P equation). A comparative evaluation of these models was
746 performed by Karathanassis et al. [156] together with the two-phase mixture
747 model in ANSYS FLUENT 14.5. The results showed that the phase-change
748 model based on the kinetic theory of gases produced accurate predictions for
749 all the cases investigated ("Super Moby Dick" nozzle [23], "Reitz" nozzle [157],
750 "Edwards" pipe blowdown [42]), while the validity of HRM and model based
751 on the R-P equation was found situational. Similar results were presented in
752 [158], which showed that the PPCM model based on the R-P equation failed in
753 reproducing the pressure undershoot phenomenon and simulating the thermal-
754 controlled phase change. For the BNL test case run 309 as an example, Figure 2
755 compares the prediction of axial void fraction and pressure profile using differ-
756 ent models with the experimental data. The void fraction provided by Le et al.
757 [41] conforms well with the measurement, while the pressure profile of Liao and
758 Lucas [40] gives the best agreement. In comparison to axial profiles, prediction
759 of the lateral distribution of void fraction is even more challenging.

760 *3.2. Pipe blowdown*

761 Jo et al. [159, 160] investigated water flashing flow from a PWR steam
762 generator (SG) by a feed water line break (FWLB) accident using the com-
763 mercial CFD code ANSYS CFX. The simplified SG model and broken position
764 is sketched in Figure 3(a). The space occupied by the tube bundle in the SG
765 secondary side was simulated with the porous medium model. The discharge
766 flow accompanying with thermal phase change was calculated by employing the
767 NHNEM two-fluid model, governing equations were solved for the liquid and
768 vapor phases separately. The gas phase consisted of discrete spherical bubbles
769 with a uniform size. The $k - \omega$ SST model was used to estimate the turbulent
770 viscosity. The phase change was driven by temperature difference and inter-
771 phase heat transfer. Transient pressure, velocity, void fraction response of the
772 SG secondary side and the broken pipe side was analyzed. Vapor was built
773 firstly at the exit of the broken pipe, and developed along the pipe wall with
774 a liquid core towards SG. The FWLB accident resulted in steep escalation of
775 the SG secondary flow velocities, especially near the broken pipe. Figure 3(b)
776 plots the mixture velocity responses at four monitoring points for the first 0.3
777 s, where the distance to the broken position decreases from point 1 to point 4.
778 At the exit of the broken nozzle (point 4), the velocity is over 100 m/s, which
779 may cause mechanical damage on some tubes. The authors investigated the
780 effect of initial state of the fluid upstream the broken pipe end, i.e. subcooled
781 water, saturated steam or saturated water-steam mixture. It was found that
782 the subcooled water non-flashing flow model gives the maximum discharge flow
783 rate, the saturated water flashing flow model the minimum, while the sub-cooled
784 water flashing flow model ranges between. In addition, the simulation results
785 were shown to have a sensitive dependence on the initial interfacial area density
786 related to the choice of gas volume fraction and bubble mean diameter.

787 Karathanassis et al. [156] presented CFD simulations of flashing flow from
788 the Edwards pipe blowdown [42] in addition to two discharge nozzles. A sketch
789 of the pipe as well as the measurement points (P1 ~ P7) is depicted in Figure
790 4. As aforementioned their numerical studies were based on the two-phase

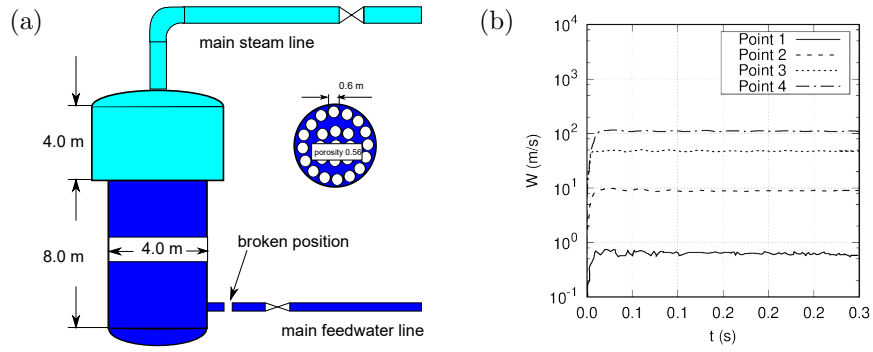


Figure 3: CFD simulation of FWLB induced discharge flow from SG [160]. (a) Simplified SG model (b) Transient velocity response at different monitoring points: Point 1 (SG center at the broken pipe level), Point 2 (first upstream point of the broken pipe in SG), Point 3 (second upstream point of the broken pipe in SG), Point 4 (center of the cross-section at the mid point of the broken pipe)

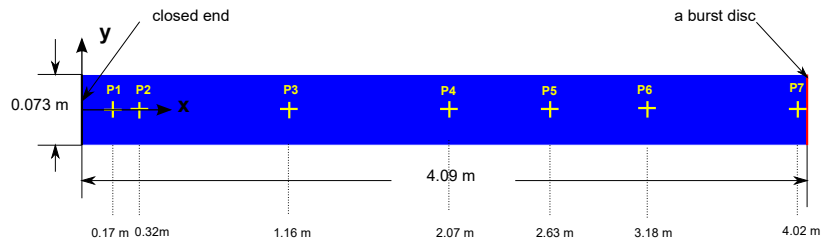


Figure 4: Sketch of the Edwards blowdown experiments [42]

791 mixture model assuming zero slip velocity. They evaluated the capability of
792 various mass-transfer rate models. The interfacial area density A_i was calculated
793 assuming a nucleation site density of $10^{13} m^{-3}$ and a bubble radius of $10^{-6} m$.
794 In other words, A_i remains constant during the phase change process, which
795 deviates obviously from the physical picture. For the blowdown case, three
796 formulations of the PPCM model based on the H-K equation, i.e. HK1, HK2,
797 HK3, were compared with the HRM model. The HK2 model computes the
798 interfacial mass flux in a way similar to Eq. 12, while in HK1 it is simplified as

$$\dot{\Gamma} = A_i C_{evap} \alpha_l \rho_l (0.195 \rho k + p_{sat} - p), \quad (18)$$

799 where C_{evap} is an empirical coefficient (= 0.001 in the investigation case). In the
800 HK3 formulation the temperature discontinuity at the interface was considered,
801 i.e.

$$\dot{\Gamma} = \frac{A_i \beta}{\sqrt{2\pi R T_{sat}}} \left(\frac{0.195 \rho k + p_{sat}}{\sqrt{T_l}} - \frac{p}{\sqrt{T_{sat}}} \right). \quad (19)$$

802 The value of 0.1 was used for the accommodation coefficient β .

803 Figures 5 (a) and (b) display the comparison of the numerical predictions of
804 transient pressure and void fraction to experimental data. One can see that all
805 the models have difficulty in capturing the flashing-inception, but the PPCM
806 model based on the H-K equation gives overall better results compared to the
807 HRM model.

808 Liao and Lucas [1] investigated the same case with the TPCM model in
809 ANSYS CFX. Apart from the different phase change model, they accounted for
810 the interphase slip velocity using the two-fluid model. A constant value of 1.0
811 mm was assumed for the bubble diameter, but the interfacial area density was
812 allowed to increase with the bubble number density as a result of phase change.
813 The comparison of the simulation results with those from [156] and experimental
814 data is shown in Figure 6. As expected, a better agreement was achieved by
815 using the TPCM model at the early stage of blowdown. The pressure undershoot
816 at the very beginning was captured well, which evidences the importance of

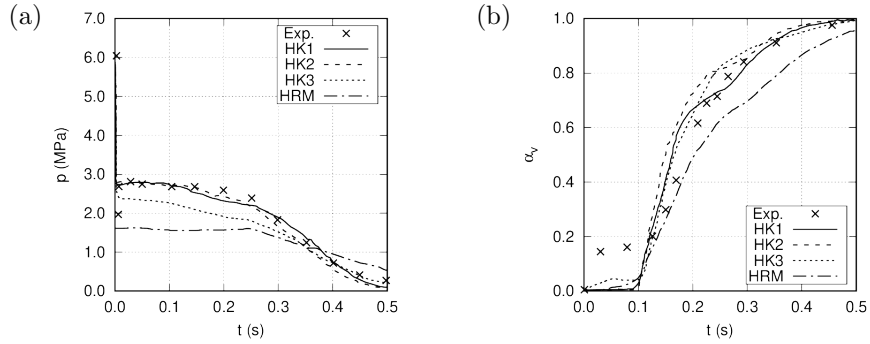


Figure 5: Edwards pipe simulation results from [156]: (a) pressure at P7 (b) void fraction at P4

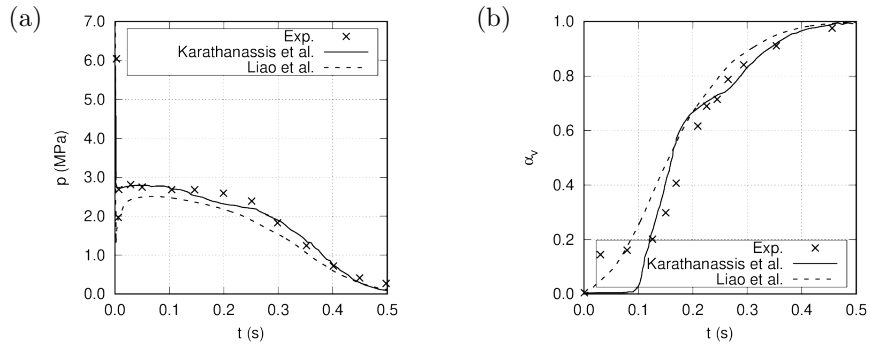


Figure 6: Edwards pipe simulation results from [1]: (a) pressure at P7 (b) void fraction at P4

817 thermal non-equilibrium at this stage.

818 3.3. Flashing-induced instability (FII)

819 As discussed in the previous section, the FII problem concerning nuclear
 820 safety analysis has been investigated intensively with experiments and system
 821 codes, whereas CFD simulations are scarce. The challenges comprise high-
 822 amplitude high-frequency waves, large geometry sizes and lack of CFD-grade
 823 experimental data. Liao et al. [1, 161, 162] presented CFD studies on the flash-
 824 ing and FII phenomenon observed at two test facilities, i.e. the AREVA INKA
 825 test facility [69] and the TUD GENEVA facility [78]. Both of them are down-

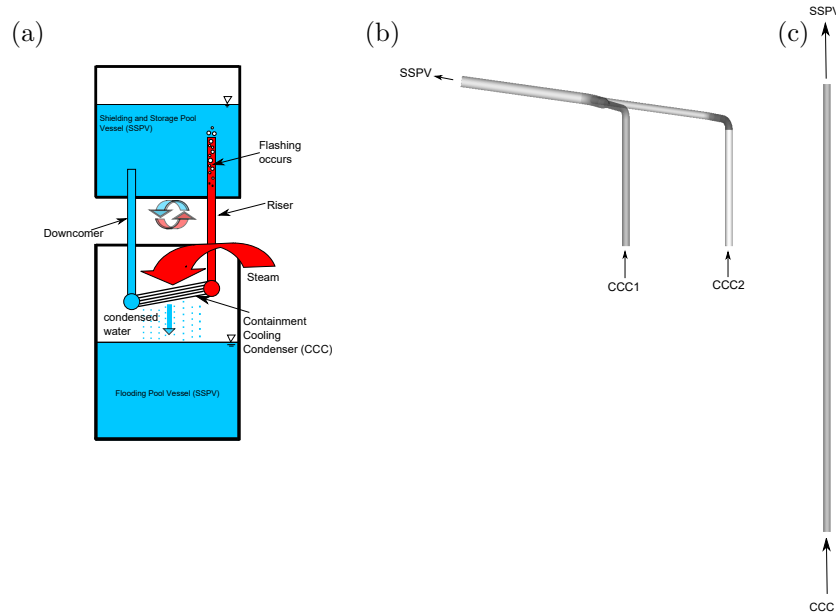


Figure 7: (a) KERENATM CCC system, (b) INKA riser [69, 161], (c) GENEVA riser [78, 162]

826 scale models of the containment cooling condenser (CCC) of the KERENATM
 827 reactor, whose function and principle is sketched in Figure 7 (a). In case of
 828 containment overpressure, steam condensed on the surface of the CCC tubes
 829 and the heat is transported by the cooling water inside the tubes via the riser
 830 to SSPV. In the INKA test facility, two sets of CCC were constructed and the
 831 riser connecting CCC1 and CCC2 with SSPV comprises of vertical and sloped
 832 pipes, see Figure 7 (b), while the GENEVA riser is a single straight pipe, which
 833 is much longer as shown in Figure 7 (c).

834 Both simulations [1, 162] were performed with the two-fluid model in AN-
 835 SYS CFX, and the computational domain was restricted to the riser for high ef-
 836 ficiency. The liquid and vapor phases were assumed in pressure equilibrium, and
 837 the TPCM was activated for interphase mass transfer. Bubbles have a spherical
 838 shape and the number density was prescribed as a constant value ($N_b = 5 \times 10^4$).
 839 Single-phase inlet was assumed, and the boundary conditions such as inlet mass
 840 flow rate, liquid temperature and outlet pressure were defined according to the

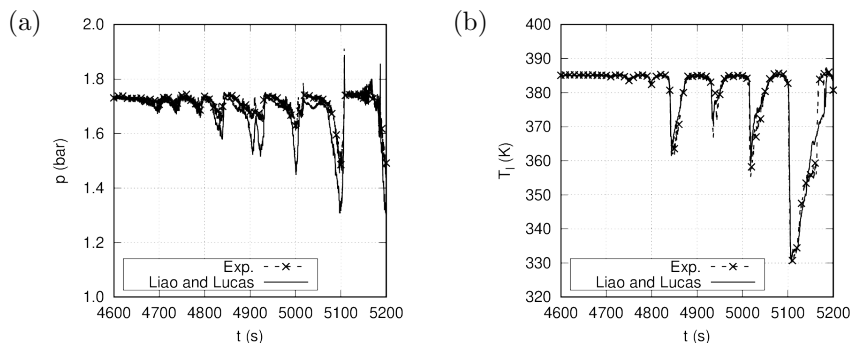


Figure 8: Comparison between simulation and measurement of pressure and temperature fluctuation in the INKA riser [1] (a) Pressure at CCC1, (b) Temperature at outlet

841 measurements. Figure 8 presents cross-section averaged pressure and tempera-
 842 ture transients inside the INKA riser, which conform well to the experimental
 843 results. The simulation showed that the onset of flashing occurs at the highest
 844 point of the domain due to low hydrostatic pressure, i.e. the top wall at the
 845 outlet, and then propagated downward to the inlets. Separated and dispersed
 846 flow was developed in the sloped and vertical pipe, respectively, and instability
 847 waves were observed at the interface, see Figure 9. As the pressure recovered
 848 the steam disappeared from bottom to top of the domain.

849 In order to reflect the non-uniform distribution of vapor bubbles at the cross
 850 section of the pipe, needle-shaped conductivity probes were installed in the central
 851 and the peripheral region (about 2/3 of the inner diameter) at the GENEVA
 852 test facility. Liao et al. [162] compared the local void fraction obtained numeri-
 853 cally and experimentally, which discovered substantial difference. As shown
 854 in Figure 10 the onset of flashing was delayed in the simulation. For example,
 855 according to the experiment at $z=3.99$ m bubbles appear at the pipe center
 856 before $t = 20$ s. On the other hand, the simulation gives non-zero void frac-
 857 tion after $t = 50$ s. Furthermore, the void fraction in the near-wall region is
 858 under-predicted, see Figure 10 (b) and 10 (d). This discrepancy is partly caused
 859 by the inaccurate prediction of bubble size, since non-drag forces representing
 860 the lateral movement of bubbles depend on it directly. The assumption of a

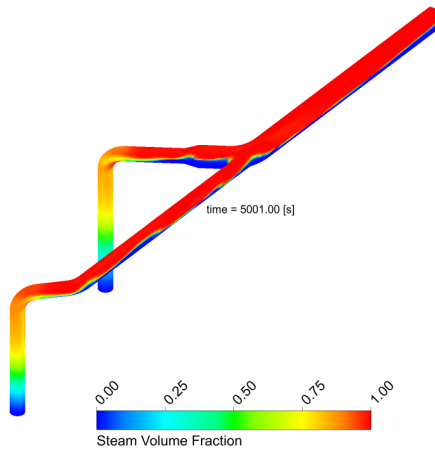


Figure 9: Steam distribution in the INKA riser [161]

861 constant bubble number density deviates from the reality, leading to a uniform
 862 local bubble size, which is either smaller or larger than the real mean value.
 863 In this case, it might be over-predicted, since the bubbles are accumulated in
 864 the pipe center due to the effect of lift force. Nevertheless, both simulation and
 865 experiment evidenced that the flashing was initiated earlier at the pipe center
 866 than the periphery. Good agreement on the central void fraction was achieved
 867 at $z = 4.99$ m (see Figure 10 (c)).

868 3.4. Pressure relief transient

869 As shown in previous examples, flashing flows represent heterogeneous mix-
 870 ture of liquid and gas with void fraction ranging from zero to one. Reliable pre-
 871 diction of local phase distribution with the CFD tool represents still a challenge
 872 relative to the cross-section averaged parameters such as pressure and tempera-
 873 ture. To improve the simulation results, it is of prime importance to reproduce
 874 the bubble size change appropriately with the model, although equivalent ef-
 875 forts are needed in modelling of bubble forces, interphase heat transfer as well as
 876 two-phase turbulence. For the purpose of model development, high-resolution
 877 high-quality experimental data are valuable. Lucas et al. [163] presented exper-
 878 iments on flash evaporation in an 8 m long vertical pipe with an inner diameter

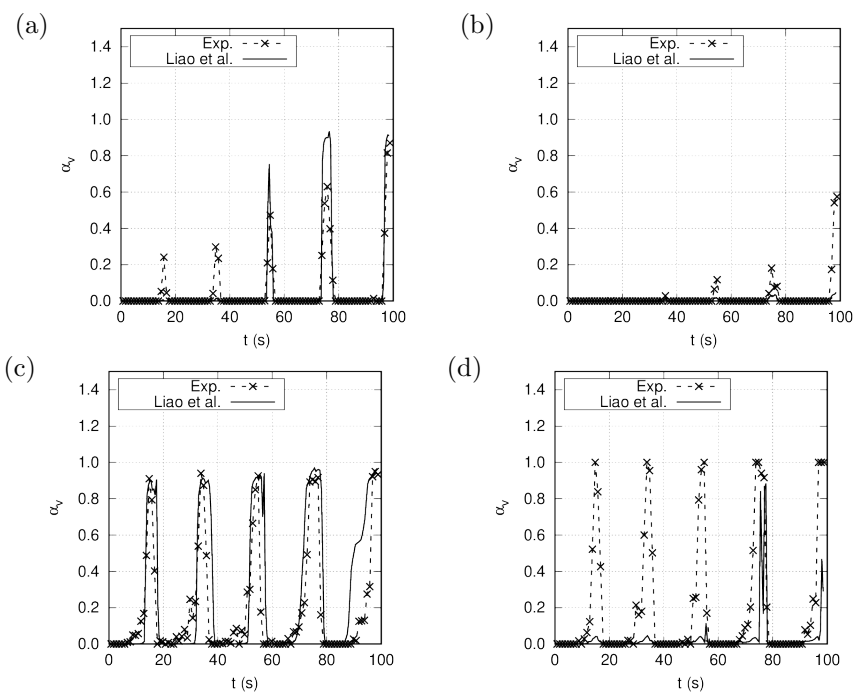


Figure 10: Comparison between simulation and measurement of local vapor void fraction inside the riser [162] (a) pipe center, $z=3.99$ m (b) 2/3 of the inner diameter, $z=3.99$ m (c) pipe center, $z=4.99$ m (d) 2/3 of the inner diameter, $z=4.99$ m

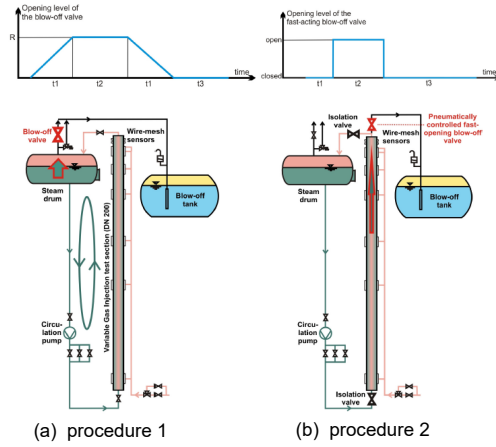


Figure 11: Pressure relief experiments at the TOPFLOW facility [163]

879 of 195.3 mm, carried out at the TOPFLOW facility. The phase change was
 880 induced by depressurization of the pipe from 1, 2, 4 and 6.5 MPa. The pres-
 881 sure relief transient and evaporation process was investigated for circulating and
 882 stagnant water, respectively, each with a different blow-off valve opening/closing
 883 procedure, see Figure 11. Detailed information on the structure of gas-liquid
 884 interfaces including spatial and temporal void fraction, bubble size distribution
 885 as well as gas velocities was obtained by using a pair of wire-mesh sensors. Mea-
 886 surements are available for different combinations of opening/closing speed and
 887 maximum opening degrees of the valve, which are represented by the parameters
 888 R , t_1 , t_2 and t_3 in Figure 11. The database is suitable for the development and
 889 validation of CFD models. Liao et al. [147, 164] presented detailed CFD stud-
 890 ies on the TOPFLOW pressure relief test cases based on the two-fluid model
 891 with thermal phase change. The main focus was put on evaluating methods for
 892 estimation of bubble diameter and interfacial area density, which vary from as-
 893 suming a constant bubble diameter or number density to using a poly-dispersed
 894 approach. The main findings are summarized as follows:

- 895 • Mono-disperse approaches fail in predicting the bubble size change and
 896 thus the lateral movement of bubbles.

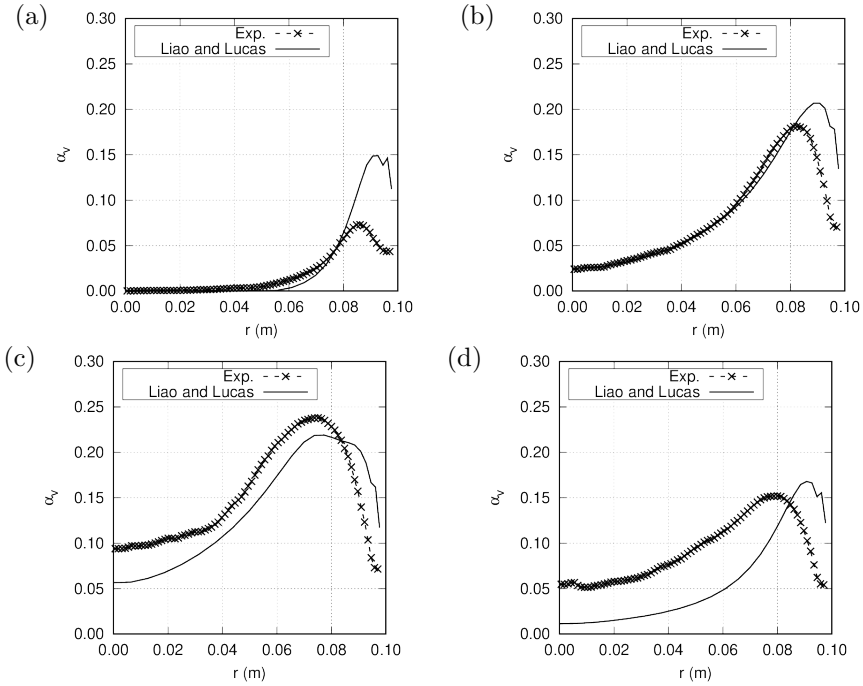


Figure 12: Comparison between simulated and measured radial void fraction profile at (a) $t = 37$ s, (b) $t = 49$ s, (c) $t = 55$ s, (d) $t = 67$ s

- 907 • The prescribed value for bubble diameter or number density affects the
908 onset of flashing as well the evaporation rate in the simulation. A too
909 large bubble diameter fails to trigger the phase change, while a too small
900 one initiates it too early.
- 901 • The contribution of wall and bulk nucleation decreases and increases re-
902 spectively with the pressure level.
- 903 • The poly-disperse approach with appropriate closures for bubble nucle-
904 ation, coalescence and breakup improves the simulation results consider-
905 ably. Radial void fraction and bubble size distribution are well captured
906 as shown in Figures 12 and 13.

907 Above CFD simulations of flashing flows are summarized in Table 3. They
908 mainly differ in whether the velocity difference between phases is considered or

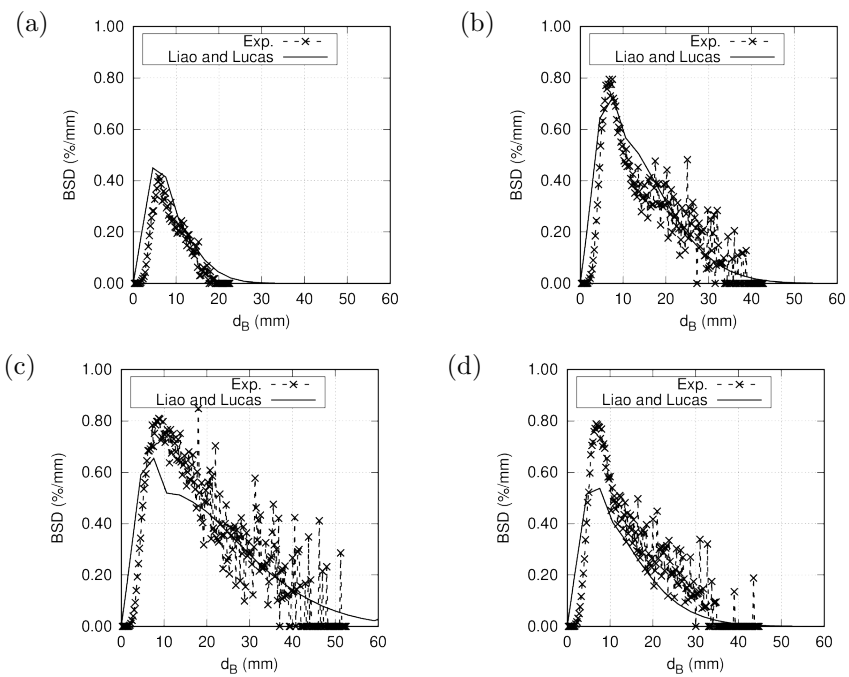


Figure 13: Comparison between simulated and measured radial void fraction profile at (a) $t = 37$ s, (b) $t = 49$ s, (c) $t = 55$ s, (d) $t = 67$ s

909 not (mixture or two-fluid model), what kind of phase change models (TPCM,
 910 PPCM, HRM or HEM) are adopted, and how to determine the interfacial area
 911 density (constant N_B , d_B , variable N_B or poly-dispersity).

References and code	Numerical models and assumptions	Experiment
[35] ANSYS CFX 4.2	<ul style="list-style-type: none"> • homogeneous mixture model • TPCM • vapor at saturation • transport equation for N_B • wall nucleation considered 	BNL nozzle [26]
[37] ANSYS FLUENT	<ul style="list-style-type: none"> • two-fluid model • non-drag forces neglected • TPCM • interface at saturation • heat transfer on vapor side neglected • transport equation for N_B • wall nucleation considered 	BNL nozzle [26]
[39] ANSYS CFX 15.0	<ul style="list-style-type: none"> • two-fluid model • drag and non-drag forces considered • TPCM • vapor and interface at saturation • transport equation for N_B • wall and bulk nucleation considered 	BNL nozzle [26]
[40] ANSYS CFX 15.0	<ul style="list-style-type: none"> • two-fluid model • drag and non-drag forces considered • TPCM • vapor and interface at saturation • prescribed value N_B 	BNL nozzle [26]
[145] NEPTUNE_CFD	<ul style="list-style-type: none"> • two-fluid model • drag and added mass force considered • TPCM 	Moby Dick nozzle [146]

	<ul style="list-style-type: none"> • vapor and interface at saturation • prescribed value für d_B • wall nucleation considered as a mass source 	
[36] ANSYS FLUENT 6.1	<ul style="list-style-type: none"> • homogeneous mixture model • PPCM based on the R-P equation 	BNL nozzle [26]
[150] ANSYS FLUENT 12.0.16	<ul style="list-style-type: none"> • homogeneous mixture model • PPCM based on the R-P equation 	Moby Dick nozzle [146] LSTF SGTR [151]
[38]	<ul style="list-style-type: none"> • homogeneous mixture model • PPCM based on the H-K equation 	BNL nozzle [26]
[41]	<ul style="list-style-type: none"> • homogeneous mixture model • slip model • PPCM based on the H-K equation 	BNL nozzle [26]
[139] in-house code	<ul style="list-style-type: none"> • homogeneous mixture model • TPCM model • PPCM based on the H-K equation 	BNL nozzle [26]
[3] OpenFOAM	<ul style="list-style-type: none"> • homogeneous mixture model • relaxation model (HRM) 	pipe flow [153, 154]
[155] NEPTUNE_CFD	<ul style="list-style-type: none"> • two-fluid model • very large drag forces • DEM model 	Moby Dick nozzle [146]
[159, 160] ANSYS CFX	<ul style="list-style-type: none"> • two-fluid model • non-drag neglected • TPCM model • prescribed value for d_B 	SG FWLB accident
[156] ANSYS FLUENT	<ul style="list-style-type: none"> • homogeneous mixture model • PPCM based on the R-P equation • PPCM based on the H-K equation • compared with the HEM, HRM model 	Moby Dick nozzle [146] "Reitz" nozzle [157] "Edwards" pipe [42]
[1] ANSYS CFX 15.0	<ul style="list-style-type: none"> • two-fluid model • TPCM 	"Edwards" pipe [42] INKA FII [69]

	<ul style="list-style-type: none"> • drag and non-drag considered • prescribed value for d_B or N_B 	
[162] ANSYS CFX 18.0	<ul style="list-style-type: none"> • two-fluid model • TPCM • drag and non-drag considered • prescribed value for N_B 	GENEVA FII [78]
[162] ANSYS CFX 18.2	<ul style="list-style-type: none"> • two-fluid model • TPCM • drag and non-drag considered • population balance model • wall and bulk nucleation considered • coalescence and breakup considered 	TOPFLOW [163]

Table 3: Summary of CFD studies on flashing flows

912 4. Conclusion

913 Although the numerical methods and models that have been used for anal-
914 ysis of flashing phenomena differ largely, there is some consensus concerning
915 following points:

- 916 • In most cases, it is necessary to account for interfacial slip appropriately
917 by using the two-fluid model.
- 918 • Non-equilibrium phase change model is more general than the relaxation
919 and equilibrium model. Thermal phase change model is superior to pres-
920 sure phase change model, when thermal non-equilibrium effects are signif-
921 icant.
- 922 • Convection has a considerable contribution to the interfacial heat transfer
923 in flashing flow, and conduction is dominant only in a short time after
924 nucleation.

- 925 • Appropriate modelling of bubble size and interfacial area density is cru-
926 cial in modelling the interphase transfer. Taking into account the poly-
927 dispersity is recommended by several researchers.
- 928 • It is difficult to reproduce the lateral motion of bubbles, where non-drag
929 forces play an important role in the interphase momentum transfer.

930 The prime challenges in CFD simulation of flashing flows arise from choosing ap-
931 propriate closure models for interphase transfer, bubble dynamics (nucleation,
932 coalescence and breakup) as well two-phase turbulence. Further efforts regard-
933 ing model improvement and data acquisition are required. Although tempera-
934 ture difference is deemed to be the predominant driving force for phase change
935 in flashing situations, the effect of pressure difference might be substantial at the
936 inception, in particular at a large pressure undershoot. In most of the simula-
937 tions, either pressure difference or temperature difference was neglected. There
938 is insufficient discussion on how to combine the two driving forces for phase
939 change properly. At high void fractions, the flow regime deviates widely from
940 bubbly flow, whereas the assumption of spherical bubbles were made in the ma-
941 jority of works. Extending a multi-scale multi-field approach, for example the
942 GENTOP model proposed by Hänsch et al. [165], to handle different bubble
943 shapes is of interest in the future. Höhne et al. [166] and Höhne and Lucas
944 [167] have demonstrated the application of this model for various boiling cases.

945 **Declarations of interest:** none.

946 **References**

- 947 [1] Y. Liao, D. Lucas, Possibilities and limitations of CFD simulation for
948 flashing flow scenarios in nuclear applications, *Energies* 10 (1) (2017)
949 139:1–22.
- 950 [2] Y. Liao, D. Lucas, Computational modelling of flash boiling flows: A
951 literature survey, *International Journal of Heat and Mass Transfer* 111
952 (2017) 246–265.

- 953 [3] D. P. Schmidt, S. Gopalakrishnan, H. Jasak, Multi-dimensional simulation
954 of thermal non-equilibrium channel flow, *International Journal of Multi-*
955 *phase Flow* 36 (4) (2010) 284–292.
- 956 [4] M. Alamgir, J. Lienhard, Correlation of pressure undershoot during hot-
957 water depressurization, *Journal of Heat Transfer* 103 (1981) 52–55.
- 958 [5] M. Maria Antony Raj, K. Kalidasa Murugavel, T. Rajaseenivasan,
959 K. Srithar, A review on flash evaporation desalination, *Desalination and*
960 *Water Treatment* 57 (29) (2016) 13462–13471.
- 961 [6] Q. Yang, B. Zhao, D. Zhang, Y. Wang, J. Yan, Experimental study on heat
962 transfer characteristics in static flash evaporation of aqueous nacl solution,
963 *International Journal of Heat and Mass Transfer* 102 (2016) 1093–1099.
- 964 [7] J. Stengler, K. Schaber, S. Mall-Gleissle, Experimental study on low tem-
965 perature desalination by flash evaporation in a novel compact chamber
966 design, *Desalination* 448 (2018) 103–112.
- 967 [8] Q. Chen, Y. Li, K. Chua, et al., Experimental and mathematical study
968 of the spray flash evaporation phenomena, *Applied Thermal Engineering*
969 130 (2018) 598–610.
- 970 [9] E. Sher, T. Bar-Kohany, A. Rashkovan, Flash-boiling atomization,
971 *Progress in energy and combustion science* 34 (4) (2008) 417–439.
- 972 [10] M. Levy, E. Sher, Transition from heterogeneous to homogeneous nucle-
973 ation in a simple structure flash-boiling atomizer, *Atomization and Sprays*
974 20 (10) 905–907.
- 975 [11] D. Ju, C. Wang, X. Qiao, J. Xiao, Z. Huang, Internal flow pattern and
976 macroscopic characteristics of a flash-boiling spray actuated through a
977 twin-orifice atomizer with low injection pressure, *Atomization and Sprays*
978 26 (4) (2016) 377–410.

- 979 [12] T. Alghamdi, S. T. Thoroddsen, J. Hernández-Sánchez, Ultra-high speed
980 visualization of a flash-boiling jet in a low-pressure environment, *International Journal of Multiphase Flow* 110 (2019) 238–255.
981
- 982 [13] A. Mansour, N. Müller, A review of flash evaporation phenomena and re-
983 sulting shock waves, *Experimental Thermal and Fluid Science* 107 (2019)
984 146–168.
- 985 [14] G. Lamanna, H. Kamoun, B. Weigand, J. Steelant, Towards a unified
986 treatment of fully flashing sprays, *International Journal of Multiphase*
987 *Flow* 58 (2014) 168–184.
- 988 [15] M. El Haj Assad, E. Bani-Hani, M. Khalil, Performance of geothermal
989 power plants (single, dual, and binary) to compensate for LHC-CERN
990 power consumption: comparative study, *Geothermal Energy* 5 (1) (2017)
991 17:1–16.
- 992 [16] S. Zheng, X. Xie, Y. Jiang, Experimental study on the flash evaporation
993 process of LiBrH₂O solution in an absorption heat pump, *International*
994 *Journal of Refrigeration* 61 (2016) 117–126.
- 995 [17] C. Danış, G. Rusu, M. Dobromir, M. Rusu, Preparation and characteri-
996 zation of CdO thin films obtained by thermal oxidation of evaporated cd
997 thin films, *Applied Surface Science* 255 (5) (2008) 2665–2670.
- 998 [18] S. Mutair, Y. Ikegami, Study and enhancement of flash evaporation desali-
999 nation utilizing the ocean thermo cline and discharged heat, *International*
1000 *Journal of Electrical and Computer Engineering* 2 (7) (2008) 1385–1392.
- 1001 [19] A. Muthunayagam, K. Ramamurthi, J. Paden, Low temperature flash
1002 vaporization for desalination, *Desalination* 180 (1-3) (2005) 25–32.
- 1003 [20] Y. Zhang, J. Wang, J. Yan, D. Chong, J. Liu, Experimental study on
1004 energy transformation and separation characteristic of circulatory flash
1005 evaporation, *International Journal of Heat and Mass Transfer* 99 (2016)
1006 862–871.

- 1007 [21] G. Wallis, Critical two-phase flow, *International Journal of Multiphase*
1008 *Flow* 6 (1-2) (1980) 97–112.
- 1009 [22] G. A. Pinhasi, A. Ullmann, A. Dayan, Modeling of flashing two-phase
1010 flow, *Reviews in Chemical Engineering* 21 (3-4) (2005) 133–264.
- 1011 [23] M. Reocreux, Contribution to the study of critical flow rates in two-phase
1012 water vapor flow, Vol. 3, US Nuclear Regulatory Commission, 1977.
- 1013 [24] V. Schrock, E. Starkman, R. Brown, Flashing flow of initially subcooled
1014 water in convergent–divergent nozzles, *Journal of Heat Transfer* 99 (2)
1015 (1977) 263–268.
- 1016 [25] E. Studsvik, Marviken full-scale critical-flow tests. volume 22. results from
1017 test 14. final report, Tech. rep., Studsvik Energiteknik AB (1982).
- 1018 [26] N. Abuaf, B. Wu, G. Zimmer, P. Saha, Study of nonequilibrium flashing
1019 of water in a converging-diverging nozzle. volume 1: experimental, Tech.
1020 rep., Brookhaven National Lab., Upton, NY (USA) (1981).
- 1021 [27] F. Moody, Maximum flow rate of a single component, two-phase mixture,
1022 *Journal of Heat Transfer* 87 (1) (1965) 134–141.
- 1023 [28] R. Henry, H. Fauske, The two-phase critical flow of one-component mix-
1024 tures in nozzles, orifices, and short tubes, *Journal of Heat Transfer* 93 (2)
1025 (1971) 179–187.
- 1026 [29] H. Richter, Separated two-phase flow model: Application to critical two-
1027 phase flow, *International Journal of Multiphase Flow* 9 (5) (1983) 511–530.
- 1028 [30] P. Saha, N. Abuaf, B. Wu, A nonequilibrium vapor generation model for
1029 flashing flows, *Journal of Heat Transfer* 106 (1984) 198–203.
- 1030 [31] B. Wu, N. Abuaf, P. Saha, Study of nonequilibrium flashing of water in a
1031 converging-diverging nozzle. volume 2. modeling, Tech. rep., Brookhaven
1032 National Lab., Upton, NY (USA) (1981).

- 1033 [32] J. Riznic, M. Ishii, N. Afgan, Mechanistic model for void distribution
1034 in flashing flow, Tech. Rep. No. CONF-8705224-1, Institut za Nuklearne
1035 Nauke Boris Kidric (1987).
- 1036 [33] I. Tiselj, S. Petelin, Modelling of the critical flashing flow in the nozzle
1037 with RELAP5 equations, in: Annual Meeting of the Nuclear Society of
1038 Slovenia, 1994.
- 1039 [34] J. Muñoz-Cobo, E. Cerezo, S. Chiva, Two phase flow modelling of flashing
1040 critical and non critical flows in converging-diverging nozzles, in: The 4th
1041 International Conference on Multiphase Flow, ICMF-4, 2001.
- 1042 [35] S. Maksic, D. Mewes, CFD-calculation of the flashing flow in pipes and
1043 nozzles, in: ASME 2002 Joint US-European Fluids Engineering Division
1044 Conference, 2002.
- 1045 [36] G. Palau-Salvador, P. González-Altozano, J. Arviza-Valverde, Numeri-
1046 cal modeling of cavitating flows for simple geometries using fluent V6. 1,
1047 Spanish Journal of Agricultural Research 5 (4) (2007) 460–469.
- 1048 [37] C. Marsh, A. O’Mahony, Three-dimensional modelling of industrial flash-
1049 ing flows, Progress in Computational Fluid Dynamics, an International
1050 Journal 9 (6-7) (2009) 393–398.
- 1051 [38] D.-M. Liu, S.-H. Liu, Y.-L. Wu, H.-Y. Xu, A thermodynamic cavitation
1052 model applicable to high temperature flow, Thermal Science 15 (suppl. 1)
1053 (2011) 95–101.
- 1054 [39] J. P. Janet, Y. Liao, D. Lucas, Heterogeneous nucleation in CFD simula-
1055 tion of flashing flows in converging-diverging nozzles, International Jour-
1056 nal of Multiphase Flow 74 (2015) 106–117.
- 1057 [40] Y. Liao, D. Lucas, 3D CFD simulation of flashing flows in a converging-
1058 diverging nozzle, Nuclear Engineering and Design 292 (2015) 149–163.

- 1059 [41] D. Q. Le, R. Mereu, G. Besagni, V. Dossena, F. Inzoli, Computational
1060 fluid dynamics modeling of flashing flow in convergent-divergent nozzle,
1061 Journal of Fluids Engineering 140 (10) 101102:1–22), year=2018, pub-
1062 lisher=American Society of Mechanical Engineers Digital Collection.
- 1063 [42] A. Edwards, T. O’Brien, Studies of phenomena connected with the de-
1064 pressurization of water reactors, J. Brit. Nucl. Energy Soc 9 (2) (1970)
1065 125–135.
- 1066 [43] K. Wolfert, The simulation of blowdown processes with condensation of
1067 thermodynamic nonequilibrium phenomena, in: OECD/NEA Specialists
1068 Mtg on Transient Two-Phase Flow, 1976.
- 1069 [44] K. Carlson, V. Ransom, R. Wagner, Application of relap5 to a pipe blow-
1070 down experiment, Tech. rep., Idaho National Engineering Lab. (1980).
- 1071 [45] G. Pinhasi, Source term modeling of gas and liquid releases from a
1072 breached pressure vessel, Ph.D. thesis, Tel-Aviv University (2001).
- 1073 [46] Y. Takeda, S. Toda, Pressure oscillation in subcooled decompression under
1074 temperature gradient, Journal of Nuclear Science and Technology 16 (7)
1075 (1979) 484–495.
- 1076 [47] N. Lafferty, V. Ransom, M. Lopez-de Bertodano, Relap5 analysis of two-
1077 phase decompression and rarefaction wave propagation under a tempera-
1078 ture gradient, Nuclear Technology 169 (1) (2010) 34–49.
- 1079 [48] O. Costa, I. Tiselj, L. Cizelj, Depressurization of vertical pipe with tem-
1080 perature gradient modeled with waha code, Science and Technology of
1081 Nuclear Installations 2012 951923:1–9), year=2012, publisher=Hindawi.
- 1082 [49] J. Lienhard, M. Alamgir, M. Trela, Early response of hot water to sudden
1083 release from high pressure, Journal of Heat Transfer 100 (1978) 473–479.
- 1084 [50] J. Bartak, A study of the rapid depressurization of hot water and the
1085 dynamics of vapour bubble generation in superheated water, International
1086 journal of multiphase flow 16 (5) (1990) 789–798.

- 1087 [51] F. D’Auria, Thermal-Hydraulics of water cooled nuclear reactors, wood-
1088 head publishing, 2017.
- 1089 [52] H. Fenech, Heat transfer and fluid flow in nuclear systems, Elsevier, 2013.
- 1090 [53] G. Brockett, H. Curet, H. W. Heiselmann, Experimental investigations of
1091 reactor system blowdown., Tech. rep., Idaho Nuclear Corp., Idaho Falls
1092 (1970).
- 1093 [54] B. Slifer, A. Rogers, Loss-of-coolant accident and emergency core cooling
1094 models for general electric boiling water reactors., Tech. rep., General
1095 Electric Co., San Jose, Calif. Atomic Power Equipment Dept. (1971).
- 1096 [55] C. Crowley, Analysis of Flashing Transient Effects During Refill: Topical
1097 Report, Vol. 88, The Commission, 1981.
- 1098 [56] G. Wang, Y. Yan, S. Shi, Z. Dang, X. Yang, M. Ishii, Experimental study
1099 of blowdown event in a pwr-type small modular reactor, Nuclear Technol-
1100 ogy 205 (1-2) (2019) 297–306.
- 1101 [57] A. Ylönen, Large break blowdown test facility study, Master’s thesis,
1102 Lappeenranta University of Technology (2008).
- 1103 [58] S. Revankar, B. Wolf, A. Vadlamani, Assessment of leak rates through
1104 steam generator tubes, Tech. rep., Purdue University, West Lafayette,
1105 IN, Final Report to Canadian Nuclear Safety Commission, PU/NE-13-11
1106 (2013).
- 1107 [59] J. Zhang, H. Yu, M. Wang, Y. Wu, W. Tian, S. Qiu, G. Su, Experimental
1108 study on the flow and thermal characteristics of two-phase leakage through
1109 micro crack, Applied Thermal Engineering 156 (2019) 145–155.
- 1110 [60] K. Tasaka, et al., ROSA-IV large scale test facility (LSTF) system de-
1111 scription for second simulated fuel assembly, Tech. rep., Japan Atomic
1112 Energy Research Institute (1990).

- 1113 [61] R. Dimenna, Semiscale steam-generator tube-rupture test results, Tech.
1114 rep., EG and G Idaho (1983).
- 1115 [62] G. Loomis, Results of the semiscale Mod-2B steam generator tube rupture
1116 test series, Tech. rep., EG and G Idaho (1985).
- 1117 [63] G. De Santi, Analysis of steam generator u-tube rupture and intentional
1118 depressurization in lobi-mod2 facility, Nuclear engineering and design
1119 126 (1) (1991) 113–125.
- 1120 [64] S. G. Lim, H. C. No, S. W. Lee, H. G. Kim, J. Cheon, J. M. Lee, S. M.
1121 Ohk, Development of stability maps for flashing-induced instability in a
1122 passive containment cooling system for ipower, Nuclear Engineering and
1123 Technology 52 (1) (2020) 37–50.
- 1124 [65] T. Schulz, Westinghouse ap1000 advanced passive plant, Nuclear Engi-
1125 neering and Design 236 (14-16) (2006) 1547–1557.
- 1126 [66] W. Zhou, B. Wolf, S. Revankar, Assessment of relap5/mod3. 3 condensa-
1127 tion models for the tube bundle condensation in the pccs of esbwr, Nuclear
1128 Engineering and Design 264 (2013) 111–118.
- 1129 [67] S. W. Lee, S. Heo, H. U. Ha, H. G. Kim, The concept of the innovative
1130 power reactor, Nuclear Engineering and Technology 49 (7) (2017) 1431–
1131 1441.
- 1132 [68] A. Bakhmet'Ev, M. Bol'Shukhin, V. Vakhrushev, A. Khizbullin,
1133 O. Makarov, V. Bezlepkin, S. Semashko, I. Ivkov, Experimental valida-
1134 tion of the cooling loop for a passive system for removing heat from the
1135 aes-2006 protective envelope design for the leningradskaya nuclear power
1136 plant site, Atomic energy 106 (3) (2009) 185–190.
- 1137 [69] S. Leyer, M. Wich, The integral test facility karlstein, Science and Tech-
1138 nology of Nuclear Installations 2012.

- 1139 [70] J. Xing, D. Song, Y. Wu, HPR1000: Advanced pressurized water reactor
1140 with active and passive safety, *Engineering* 2 (1) (2016) 79–87.
- 1141 [71] E. Wissler, H. Isbin, N. Amundson, Oscillatory behavior of a two-phase
1142 natural-circulation loop, *AIChE Journal* 2 (2) (1956) 157–162.
- 1143 [72] A. Manera, T. van der Hagen, Stability of natural-circulation-cooled boil-
1144 ing water reactors during startup: experimental results, *Nuclear technol-
1145 ogy* 143 (1) (2003) 77–88.
- 1146 [73] M. Furuya, F. Inada, T. van der Hagen, Flashing-induced density wave
1147 oscillations in a natural circulation bwr—mechanism of instability and
1148 stability map, *Nuclear engineering and design* 235 (15) (2005) 1557–1569.
- 1149 [74] C. Marcel, M. Rohde, T. van der Hagen, Experimental and numerical
1150 investigations on flashing-induced instabilities in a single channel, *Exper-
1151 imental thermal and fluid science* 33 (8) (2009) 1197–1208.
- 1152 [75] C. Marcel, M. Rohde, T. van der Hagen, Experimental investigations on
1153 flashing-induced instabilities in one and two-parallel channels: A com-
1154 parative study, *Experimental Thermal and Fluid Science* 34 (7) (2010)
1155 879–892.
- 1156 [76] H. Khartabil, A flashing driven moderator cooling system for candu reac-
1157 tors: Experimental and computational results, *Tech. rep.* (2000).
- 1158 [77] S.-K. Yang, Stability of flashing-driven natural circulation in a passive
1159 moderator cooling system for canadian scwr, *Nuclear engineering and de-
1160 sign* 276 (2014) 259–276.
- 1161 [78] T. Cloppenborg, C. Schuster, A. Hurtado, Two-phase flow phenomena
1162 along an adiabatic riser—an experimental study at the test-facility geneva,
1163 *International Journal of Multiphase Flow* 72 (2015) 112–132.
- 1164 [79] J. Andersen, F. Inada, L. Klebanov, TRACG analyses of flashing insta-
1165 bility during start-up, in: *The 21st International Conference on Nuclear
1166 Engineering, ICON-3, 1995.*

- 1167 [80] A. Manera, U. Rohde, H.-M. Prasser, T. van der Hagen, Modeling of
1168 flashing-induced instabilities in the start-up phase of natural-circulation
1169 bwrns using the two-phase flow code focal, Nuclear Engineering and Design
1170 235 (14) (2005) 1517–1535.
- 1171 [81] Y. Kozmenkov, U. Rohde, A. Manera, Validation of the relap5 code for the
1172 modeling of flashing-induced instabilities under natural-circulation condi-
1173 tions using experimental data from the circus test facility, Nuclear engi-
1174 neering and design 243 (2012) 168–175.
- 1175 [82] Q. Wang, P. Gao, X. Chen, Z. Wang, Y. Huang, An investigation on
1176 flashing-induced natural circulation instabilities based on relap5 code, An-
1177 nals of Nuclear Energy 121 (2018) 210–222.
- 1178 [83] J. Jeong, K. Ha, B. Chung, W. Lee, Development of a multi-dimensional
1179 thermal-hydraulic system code, mars 1.3. 1, Annals of Nuclear Energy
1180 26 (18) (1999) 1611–1642.
- 1181 [84] H. K. Fauske, Contribution to the theory of two-phase, one-component
1182 critical flow, Tech. rep., Argonne National Lab., Ill. (1962).
- 1183 [85] H. Isbin, J. Moy, A. Da Cruz, Two-phase, steam-water critical flow,
1184 AIChE Journal 3 (3) (1957) 361–365.
- 1185 [86] F. Zaloudek, The low pressure critical discharge of steam-water mixtures
1186 from pipes, Tech. rep., General Electric Co. Hanford Atomic Products
1187 Operation, Richland, Wash. (1961).
- 1188 [87] D. W. Faletti, R. Moulton, Two-phase critical flow of steam-water mix-
1189 tures, AIChE Journal 9 (2) (1963) 247–253.
- 1190 [88] F. Inada, O. T., Thermo-hydraulic instability of natural circulation BWRs
1191 (explanation on instability mechanisms at start-up by homogeneous and
1192 thermo-dynamic equilibrium model considering flashing effect), in: Inter-
1193 national Conference on New Trends in Nuclear System Thermohydraulics,
1194 1994.

- 1195 [89] D. Van Bragt, W. De Kruijf, A. Manera, T. van der Hagen, H. van Dam,
1196 Analytical modeling of flashing-induced instabilities in a natural circula-
1197 tion cooled boiling water reactor, *Nuclear engineering and design* 215 (1-2)
1198 (2002) 87–98.
- 1199 [90] S. Levy, Prediction of two-phase critical flow rate, *Journal of Heat Transfer*
1200 87 (1) (1965) 53–57.
- 1201 [91] R. Hu, M. Kazimi, Flashing-induced instability analysis and the start-up
1202 of natural circulation boiling water reactors, *Nuclear technology* 176 (1)
1203 (2011) 57–71.
- 1204 [92] F. Inada, M. Furuya, A. Yasuo, Thermo-hydraulic instability of boiling
1205 natural circulation loop induced by flashing (analytical consideration),
1206 *Nuclear Engineering and Design* 200 (1-2) (2000) 187–199.
- 1207 [93] A. Attou, M. Giot, J.-M. Seynhaeve, Modelling of steady-state two-phase
1208 bubbly flow through a sudden enlargement, *International journal of heat*
1209 *and mass transfer* 40 (14) (1997) 3375–3385.
- 1210 [94] J. Bouré, Critical flow phenomenon with reference to two-phase flow and
1211 nuclear reactor systems, in: *Thermal and hydraulic aspects of nuclear*
1212 *reactor safety*. Vol. I, 1977.
- 1213 [95] H. C. Simpson, R. Silver, Theory of one-dimensional, two-phase homoge-
1214 neous non-equilibrium flow, in: *Institute of Mechanical Engineers Sympo-*
1215 *sium on Two-phase Fluid Flow*, 1962.
- 1216 [96] C. Lackme, Thermodynamics of critical two-phase discharge from long
1217 pipes of initially subcooled water, in: *ICHMT Digital Library Online*,
1218 *Begel House Inc.*, 1982.
- 1219 [97] S. Lee, V. Schrock, Critical two-phase flow in pipes for subcooled stag-
1220 nation states with a cavity flooding incipient flashing model, *Journal of*
1221 *Heat Transfer* 112 (4) (1990) 1032–1040.

- 1222 [98] E. Elias, P. Chambre, Flashing inception in water during rapid decom-
1223 pression, *Journal of Heat Transfer* 115 (1) (1993) 231–238.
- 1224 [99] S. Levy, D. Abdollahian, Homogeneous non-equilibrium critical flow
1225 model, *International Journal of Heat and Mass Transfer* 25 (6) (1982)
1226 759–770.
- 1227 [100] J. J. Schröder, N. Vuxuan, Homogeneous non-equilibrium two-phase criti-
1228 cal flow model, *Chemical Engineering & Technology* 10 (1) (1987) 420–426.
- 1229 [101] E. Bauer, G. Houdayer, H. Sureau, A non-equilibrium axial flow model
1230 in application to loss-of-accident analysis. the cystere system code, in:
1231 OECD/NEA Specialists Meeting on Transient Two-phase flow, Atomic
1232 Energy of Canada, 1976.
- 1233 [102] P. Kroeger, Application of a non-equilibrium drift flux model to two-phase
1234 blowdown experiments, Tech. rep., Brookhaven National Lab., Upton, NY
1235 (USA) (1976).
- 1236 [103] Z. Bilicki, J. Kestin, Physical aspects of the relaxation model in two-phase
1237 flow, *Proceedings of the Royal Society of London. A. Mathematical and
1238 Physical Sciences* 428 (1875) (1990) 379–397.
- 1239 [104] K. Neroorkar, S. Gopalakrishnan, R. Grover Jr, D. Schmidt, Simulation
1240 of flash boiling in pressure swirl injectors, *Atomization and Sprays* 21 (2)
1241 (2011) 179–188.
- 1242 [105] E. T. Baldwin, R. O. Grover Jr, S. E. Parrish, D. J. Duke, K. E. Matusik,
1243 C. F. Powell, A. L. Kastengren, D. P. Schmidt, String flash-boiling in
1244 gasoline direct injection simulations with transient needle motion, *Inter-
1245 national Journal of Multiphase Flow* 87 (2016) 90–101.
- 1246 [106] K. Saha, S. Som, M. Battistoni, Investigation of homogeneous relaxation
1247 model parameters and their implications for gasoline injectors, *Atomiza-
1248 tion and Sprays* 27 (4) (2017) 345–365.

- 1249 [107] H. Guo, Y. Li, B. Wang, H. Zhang, H. Xu, Numerical investigation on
1250 flashing jet behaviors of single-hole gdi injector, *International Journal of*
1251 *Heat and Mass Transfer* 130 (2019) 50–59.
- 1252 [108] C. Lackme, Incompleteness of the flashing of a supersaturated liquid and
1253 sonic ejection of the produced phases, *International Journal of Multiphase*
1254 *Flow* 5 (2) (1979) 131–141.
- 1255 [109] M. De Lorenzo, P. Lafon, J.-M. Seynhaeve, Y. Bartosiewicz, Benchmark
1256 of delayed equilibrium model (dem) and classic two-phase critical flow
1257 models against experimental data, *International Journal of Multiphase*
1258 *Flow* 92 (2017) 112–130.
- 1259 [110] U. Rohatgi, E. Reshotko, Non-equilibrium one-dimensional two-phase flow
1260 in variable area channels, in: *Non-equilibrium two-phase flows; Proceed-*
1261 *ings of the Winter Annual Meeting, 1975.*
- 1262 [111] V. Blinkov, O. Jones, B. Nigmatulin, Nucleation and flashing in noz-
1263 zles—2. comparison with experiments using a five-equation model for va-
1264 por void development, *International Journal of Multiphase Flow* 19 (6)
1265 (1993) 965–986.
- 1266 [112] P. Deligiannis, J. Cleaver, The role of nucleation in the initial phases of
1267 a rapid depressurization of a subcooled liquid, *International Journal of*
1268 *Multiphase Flow* 16 (6) (1990) 975–984.
- 1269 [113] E. Elias, S. Levy, P. Chambré, A mechanistic non-equilibrium model for
1270 two-phase critical flow, *International Journal of Multiphase Flow* 10 (1)
1271 (1984) 21–40.
- 1272 [114] H. Atajafari, M. Nematollahi, M. Hashemi-Tilehnoee, N. Rafiee, et al.,
1273 Validation of RELAP5/MOD3. 2 code for flashing-induced instabilities in
1274 a single channel, *World Journal of Nuclear Science and Technology* 5 (1)
1275 (2015) 6–17.

- 1276 [115] M. Wein, Numerische simulation von kritischen und nahkritischen
1277 zweiphasenströmungen mit thermischen und fluiddynamischen nichtgle-
1278 ichgewichtseffekten, Ph.D. thesis, Technical University of Dresden (2002).
- 1279 [116] J. Leung, A generalized correlation for one-component homogeneous equi-
1280 librium flashing choked flow, *AICHE Journal* 32 (10) (1986) 1743–1746.
- 1281 [117] R. Hu, J. Zhao, S.-P. Kao, M. Kazimi, Thermal-hydraulic stability analysis
1282 of natural circulation bwrs, in: *International Congress on Advances in
1283 Nuclear Power Plants (ICAPP 2007)*, 2007.
- 1284 [118] M. Podowski, Modeling and analysis of two-phase flow instabilities, in:
1285 *The 14th International Topical Meeting on Nuclear Reactor Thermalhy-
1286 draulics, NURETH-10*, 2003.
- 1287 [119] P. Downar-Zapolski, Z. Bilicki, L. Bolle, J. Franco, The non-equilibrium
1288 relaxation model for one-dimensional flashing liquid flow, *International
1289 journal of multiphase flow* 22 (3) (1996) 473–483.
- 1290 [120] H. Kato, H. Kayano, Y. Kageyama, A consideration of thermal effect
1291 on cavitation bubble growth, Tech. rep., American Society of Mechanical
1292 Engineers, New York, NY (United States) (1994).
- 1293 [121] D. P. Schmidt, Cavitation in diesel fuel injector nozzles, Ph.D. thesis,
1294 University of Wisconsin–Madison (1997).
- 1295 [122] S. Yin, N. Wang, H. Wang, Nucleation and flashing inception in flashing
1296 flows: A review and model comparison, *International Journal of Heat and
1297 Mass Transfer* 146 (2020) 118898.
- 1298 [123] Z. Bilicki, R. Kwidziński, S. A. Mohammadein, Evaluation of the relax-
1299 ation time of heat and mass exchange in the liquid-vapour bubble flow,
1300 *International Journal of Heat and Mass Transfer* 39 (4) (1996) 753–759.
- 1301 [124] S. Mohammadein, The derivation of thermal relaxation time between two-
1302 phase bubbly flow, *Heat and Mass Transfer* 42 (5) (2006) 364–369.

- 1303 [125] F. Dobran, Nonequilibrium modeling of two-phase critical flows in tubes,
1304 Journal of Heat Transfer 109 (1987) 731–738.
- 1305 [126] M. S. Plesset, S. A. Zwick, The growth of vapor bubbles in superheated
1306 liquids, Journal of Applied Physics 25 (4) (1954) 493–500.
- 1307 [127] E. Ruckenstein, On heat transfer between vapour bubbles in motion and
1308 the boiling liquid from which they are generated, Chemical Engineering
1309 Science 10 (1-2) (1959) 22–30.
- 1310 [128] N. Zuber, J. Findlay, Average volumetric concentration in two-phase flow
1311 systems, Journal of Heat Transfer 87 (4) (1965) 453–468.
- 1312 [129] H. Forster, N. Zuber, Growth of a vapor bubble in a superheated liquid,
1313 Journal of Applied Physics 25 (4) (1954) 474–478.
- 1314 [130] Y. Liao, D. Lucas, Evaluation of interfacial heat transfer models for flash-
1315 ing flow with two-fluid cfd, Fluids 3 (2) (2018) 38.
- 1316 [131] O. Jones Jr, N. Zuber, Bubble growth in variable pressure fields, Journal
1317 of Heat Transfer 100 (1978) 453–459.
- 1318 [132] K. Ardron, A two-fluid model for critical vapour-liquid flow, International
1319 Journal of Multiphase Flow 4 (3) (1978) 323–337.
- 1320 [133] W. Rivard, J. Travis, A nonequilibrium vapor production model for critical
1321 flow, Nuclear Science and Engineering 74 (1) (1980) 40–48.
- 1322 [134] W. Ranz, W. Marshall, Evaporation from drops: Ii. chem, Chemical En-
1323 gineering Progress 48 (4) (1952) 173–180.
- 1324 [135] C. Schwellnus, A study of a general one-dimensional two-fluid critical flow
1325 model, Master’s thesis, McMaster University (November 1988).
- 1326 [136] R. Dagan, E. Elias, E. Wacholder, S. Olek, A two-fluid model for critical
1327 flashing flows in pipes, International journal of multiphase flow 19 (1)
1328 (1993) 15–25.

- 1329 [137] S. Olek, Y. Zvirin, E. Elias, Bubble growth predictions by the hyperbolic
1330 and parabolic heat conduction equations, *Wärme-und Stoffübertragung*
1331 25 (1) (1990) 17–26.
- 1332 [138] D. Bestion, Extension of CFD codes application to two-phase flow safety
1333 problems, *Nuclear Engineering and Technology* 42 (4) (2010) 365–376.
- 1334 [139] M.-S. Jin, C.-T. Ha, W.-G. Park, Numerical study on heat transfer effects
1335 of cavitating and flashing flows based on homogeneous mixture model,
1336 *International Journal of Heat and Mass Transfer* 109 (2017) 1068–1083.
- 1337 [140] D. Labuntzov, B. Lolchugin, V. Golovin, E. Zakharova, L. Vladimirova,
1338 High speed camera investigation of bubble growth for saturated water
1339 boiling in a wide range of pressure variations, *Thermophys. High Temp.*
1340 2 (1964) 446–453.
- 1341 [141] M. Blander, J. L. Katz, Bubble nucleation in liquids, *AIChE Journal*
1342 21 (5) (1975) 833–848.
- 1343 [142] Y. Aleksandrov, G. Voronov, V. Gorbunkow, N. Delone, Y. Nechayev,
1344 Bubble chambers (translated by Scripta Technica, Inc.) (1962).
- 1345 [143] I. Ansys, ANSYS CFX-solver theory guide, 2012.
- 1346 [144] Y. Liao, T. Ma, L. Liu, T. Ziegenhein, E. Krepper, D. Lucas, Eulerian
1347 modelling of turbulent bubbly flow based on a baseline closure concept,
1348 *Nuclear Engineering and Design* 337 (2018) 450–459.
- 1349 [145] S. Mimouni, M. Boucker, J. Laviéville, A. Guelfi, D. Bestion, Modelling
1350 and computation of cavitation and boiling bubbly flows with the NEP-
1351 TUNE_CFD code, *Nuclear Engineering and Design* 238 (3) (2008) 680–
1352 692.
- 1353 [146] M. Robert, M. Farvacque, M. Parent, B. Faydide, CATHARE 2 V2.5: A
1354 fully validated CATHARE version for various applications, in: *The 14th*

- 1355 International Topical Meeting on Nuclear Reactor Thermalhydraulics,
1356 NURETH-10, 2003.
- 1357 [147] Y. Liao, D. Lucas, Numerical analysis of flashing pipe flow using a pop-
1358 ulation balance approach, *International Journal of Heat and Fluid Flow*
1359 77 (2019) 299–313.
- 1360 [148] A. K. Singhal, M. M. Athavale, H. Li, Y. Jiang, Mathematical basis and
1361 validation of the full cavitation model, *J. Fluids Eng.* 124 (3) (2002) 617–
1362 624.
- 1363 [149] G. H. Schnerr, J. Sauer, Physical and numerical modeling of unsteady
1364 cavitation dynamics, in: *The 4th International Conference on Multiphase*
1365 *Flow, ICMF-4*, 2001.
- 1366 [150] M. Ishigaki, T. Watanabe, H. Nakamura, Numerical simulation of two-
1367 phase critical flow with the phase change in the nozzle tube, *Journal of*
1368 *Power and Energy Systems* 6 (2) (2012) 264–274.
- 1369 [151] T. Kuroda, T. Watanabe, Y. Kukita, Break flow modeling for a steam
1370 generator tube rupture (sgtr) incident in a pressurized water reactor (pwr),
1371 Tech. rep., Japan Atomic Energy Research institute (1993).
- 1372 [152] W. H. Lee, A pressure iteration scheme for two-phase flow modeling, in:
1373 *Multiphase Transport: Fundamentals, Reactor safety, Applications*, 1980.
- 1374 [153] L. Tikhonenko, L. Kevorkov, S. Lutovinov, Investigation of local parame-
1375 ters of critical flow of hot water in straight pipes with a sharp inlet edge,
1376 *Thermal Engineering* 25 (2) (1978) 40–43.
- 1377 [154] H. Fauske, The discharge of saturated water through tubes, in: *Chemical*
1378 *Engineering Progress Symposium Series*, 1965.
- 1379 [155] M. Duponcheel, J.-M. Seynhaeve, Y. Bartosiewicz, Implementation and
1380 assessment of the delayed equilibrium model for computing flashing choked

- 1381 flows in a multi-field cfd code, in: The 14th International Topical Meeting
1382 on Nuclear Reactor Thermalhydraulics, NURETH-16, 2015.
- 1383 [156] I. Karathanassis, P. Koukouvinis, M. Gavaises, Comparative evaluation
1384 of phase-change mechanisms for the prediction of flashing flows, Interna-
1385 tional Journal of Multiphase Flow 95 (2017) 257–270.
- 1386 [157] R. D. Reitz, A photographic study of flash-boiling atomization, Aerosol
1387 Science and Technology 12 (3) (1990) 561–569.
- 1388 [158] Y. Liao, D. Lucas, On numerical simulation of flashing flows, in: The 14th
1389 International Topical Meeting on Nuclear Reactor Thermalhydraulics,
1390 NURETH-18, 2019.
- 1391 [159] J. C. Jo, J. J. Jeong, B. J. Yun, F. Moody, Numerical prediction of a
1392 flashing flow of saturated water at high pressure, Nuclear Engineering
1393 and Technology 50 (7) (2018) 1173–1183.
- 1394 [160] J. C. Jo, J. J. Jeong, B. J. Yun, J. Kim, Numerical analysis of sub-
1395 cooled water flashing flow from a pressurized water reactor steam genera-
1396 tor through an abruptly broken main feed water pipe, Journal of Pressure
1397 Vessel Technology 141 (4) (2019) 044501:1–10.
- 1398 [161] Y. Liao, D. Lucas, E. Krepper, R. Rzehak, CFD simulation of flash-
1399 ing boiling flow in the containment cooling condensers (CCC) system
1400 of kerenaTM reactor, in: 21st International Conference on Nuclear En-
1401 gineering, ICONE-21, American Society of Mechanical Engineers Digital
1402 Collection, 2013.
- 1403 [162] Y. Liao, C. Schuster, S. Hu, D. Lucas, CFD modelling of flashing insta-
1404 bility in natural circulation cooling systems, in: The 21st International
1405 Conference on Nuclear Engineering, ICONE-26, American Society of Me-
1406chanical Engineers Digital Collection, 2018.

- 1407 [163] D. Lucas, M. Beyer, L. Szalinski, Experiments on evaporating pipe flow,
1408 in: The 14th International Topical Meeting on Nuclear Reactor Thermal-
1409 hydraulics, NURETH-14, 2011.
- 1410 [164] Y. Liao, D. Lucas, E. Krepper, R. Rzehak, Flashing evaporation under
1411 different pressure levels, Nuclear Engineering and Design 265 (2013) 801–
1412 813.
- 1413 [165] S. Hänsch, D. Lucas, E. Krepper, T. Höhne, A multi-field two-fluid con-
1414 cept for transitions between different scales of interfacial structures, In-
1415 ternational Journal of Multiphase Flow 47 (2012) 171–182.
- 1416 [166] T. Höhne, E. Krepper, D. Lucas, G. Montoya, A multiscale approach sim-
1417 ulating boiling in a heated pipe including flow pattern transition, Nuclear
1418 Technology 205 (1-2) (2019) 48–56.
- 1419 [167] T. Höhne, D. Lucas, A multiscale approach simulating generic pool boil-
1420 ing, Nuclear Science and Engineering (2020) 1–14.